REPORT

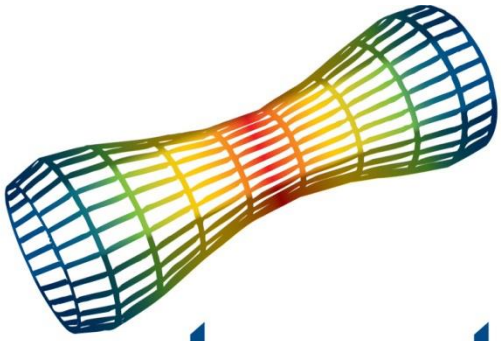

aquastructures

Safety through technology

LOADS ON IMPERMABLE NETS AND LARGE VOLUME OBJECTS IN AQUASIM

REPORT NO. TR-FOU-2328-5

REVISION NO. 05

AQUASTRUCTURES

Report title:	LOADS ON IMPERMEABLE NETS AND LARGE VOLUME OBJECTS IN AQUASIM
Project no.:	2328
Client:	Norges Forskningsråd
Approved by:	Are Johan Berstad
Date of first issue:	09.12.2019
Organisational unit:	Research and development
Number of pages:	42
Availability:	Unrestricted distribution
Work carried out by:	Are Johan Berstad
Work verified by:	Line Fludal Heimstad
Indexing terms:	Finite Element Analysis Hydrodynamic hydrostatic MacCamy and Fuchs VS numerical

Summary:

This document describes how hydrostatic and hydrodynamic forces are calculated in AquaSim where impermeable nets, or shell elements, are distributed around an object.

Further, verifications of the numerical calculation of diffraction forces by comparing MacCamy Fuchs and numerical solution to analytical solutions for cases where the water is acting on a stiff object. The report outlines a load model for a fully flexible tarp and shows how to combine this load model with the diffraction load model to obtain a hybrid load model applicable for tubes or lice skirts.

1	09.12.2019	AJB	ISH
2	19.05.2020	AJB	LFH
3	29.05.2020	AJB	LFH
4	06.08.2020	AJB	LFH
5	19.01.2021	AJB	LFH
Revision no.	*Date:*	*Work done by:*	*Work verified by:*

Table of Content

1. INTRODUCTION 1

2. SEA LOADS TO OBJECTS IN WATER 1

2.1. Hydrostatic forces. 1

2.1.1. Buoyancy 1

2.2. Current and viscous forces 2

2.2.1. Forces from current flow around cylinder 2

2.2.2. Effect of deformation of the cylinder 6

2.3. Waves 7

2.3.1.1. Froude Krylov force 10

2.3.1.2. Diffraction force 10

2.3.1.3. The splash-zone 11

2.4. Hydrodynamic forces to a flexible panel 12

2.5. Added mass and damping 14

2.5.1. Hydrodynamic added mass and damping 14

2.5.2. (Added) mass and Damping 14

2.6. Wave drift forces 14

2.7. Hybrid load model 14

2.8. In and out of the waterline 15

2.9. Waves and current combined 15

3. CASE STUDIES 15

3.1. Vertical cylinder, stiff 15

3.2. Case compared to reflection from a wall 18

3.3. Flexible tube net 20

3.3.1. Testing and comparison current 23

3.3.2. Testing and comparison regular waves with current 28

3.3.3. Sensitivity of load model 33

3.3.4. Sensitivity of added mass 35

3.3.5. Results discussion 37

4. CONCLUSION 38

5. REFERENCES 39

1. INTRODUCTION

In AquaSim the diffraction forces on an object can be estimated either by MacCamy Fuchs theory or by a numerical estimate, and the user can scale these load components to obtain an approximation for flexible tarp. (A tarp or tarpaulin, is a large sheet of strong, flexible, water-resistant, or waterproof material, often cloth such as canvas or polyester coated with polyurethane or made of plastics such as polyethylene.)

This report shows how hydrostatic and hydrodynamic forces are calculated in AquaSim where impermeable net or shell elements are distributed around an object.

This report verifies the numerical calculation of diffraction forces by comparing MacCamy Fuchs and numerical solutions to analytical solutions for cases where the water is acting on a stiff object. The report outlines a load model for a fully flexible tarp and shows how to combine this load model with the diffraction load model to obtain a hybrid load model applicable for tubes or lice skirts. This model is compared to model test results for a tube. The results are discussed in light of the load model.

2. SEA LOADS TO OBJECTS IN WATER

For introduction, an overview of forces to objects in water is given firstly.

2.1. Hydrostatic forces.

Consider an object floating in water as shown in Figure 1.

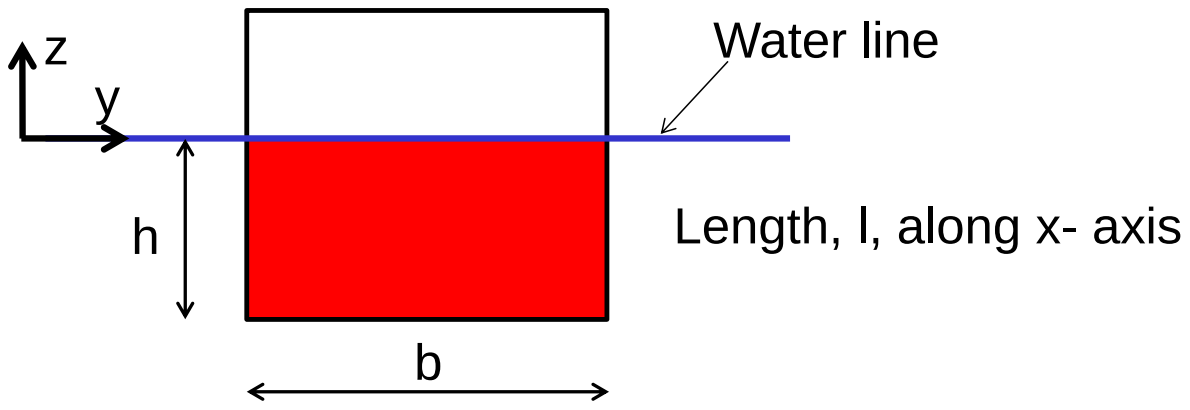

Figure 1 Rectangular object seen in the *y-z* plane.

2.1.1. Buoyancy

The forces acting from the water to the structure is the integral of the fluid pressure around the object. Define an orthonormal coordinate system where the x- axis is along the object in the horizontal plane, the z- axis is upwards with origin at the mean water line. Hydrostatic pressure increase downwards in a fluid and the hydrostatic pressure at a given point in a fluid (see e.g. http://en.wikipedia.org/wiki/Fluid_statics) can be found as:

$$p = -\rho g z + p_{atm}$$

Equation 1

Where ρ is the density of water, g is gravity, z is the vertical location (origin at free surface and axis pointing upwards) p_{atm} is the atmospheric pressure in air at the free surface.

Assume the fluid is non-viscous. Then a force originating by fluid pressure will be directed normal to the surface. Introducing this to the case seen in Figure 1 it is seen that the net horizontal force is 0 due to symmetry and the net vertical force is

$$F = \rho g h b l$$

Equation 2

Where F is positive upwards and l is the length out of the plane seen in Figure 1 and h and b are as defined in the figure. Equation 1 can be rewritten to

$$F = \rho g V$$

Equation 3

Where V is the submerged volume. As seen this is in accordance with Archimedes principle (http://en.wikipedia.org/wiki/Archimedes%27_principle).

Consider a case where there is just a net without closed bottom as seen in Figure 2. In this case the static pressure from water will be equal on the inside and the outside.

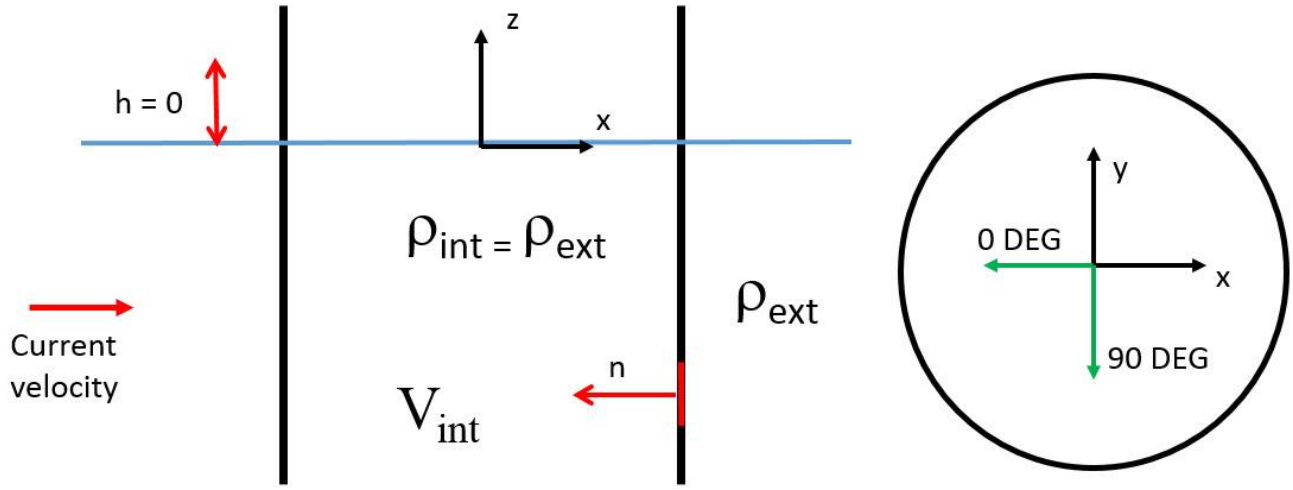

Figure 2 Impermeable net in current flow.

2.2. Current and viscous forces

For regular fish farms based on twine nets, the forces caused by current are normally the largest environmental load. The physics of impermeable nets are different, and the flow cannot pass through the object. This section exemplifies this with a cylinder which is a very relevant shape for aquaculture units.

2.2.1. Forces from current flow around cylinder

Impermeable nets may also be open at the top and bottom. For example, skirts to avoid lice. This is shown in Figure 2. In this case, the static pressure inside will be equal to the static pressure outside the net.

Consider a current velocity approaching along the x- axis. The current flow around a cylindrical net is approximated by the current flow around a cylinder. A flow around a cylinder will introduce a velocity field as shown in Figure 3. This velocity field will introduce a pressure field to the cylinder.

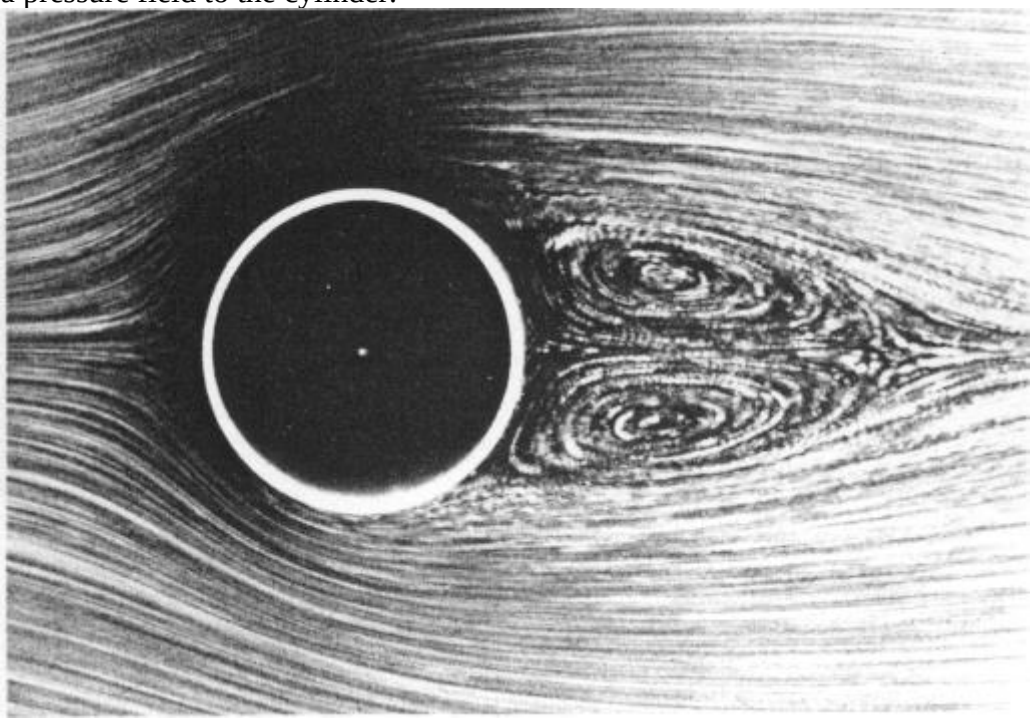

Figure 3 Streamlines of flow passing cylinder (Barkley 2006)

The pressure-field to the cylinder, which integrated around the circumference leads to the drag force on the cylinder. The pressure-field may look as shown in Figure 4.

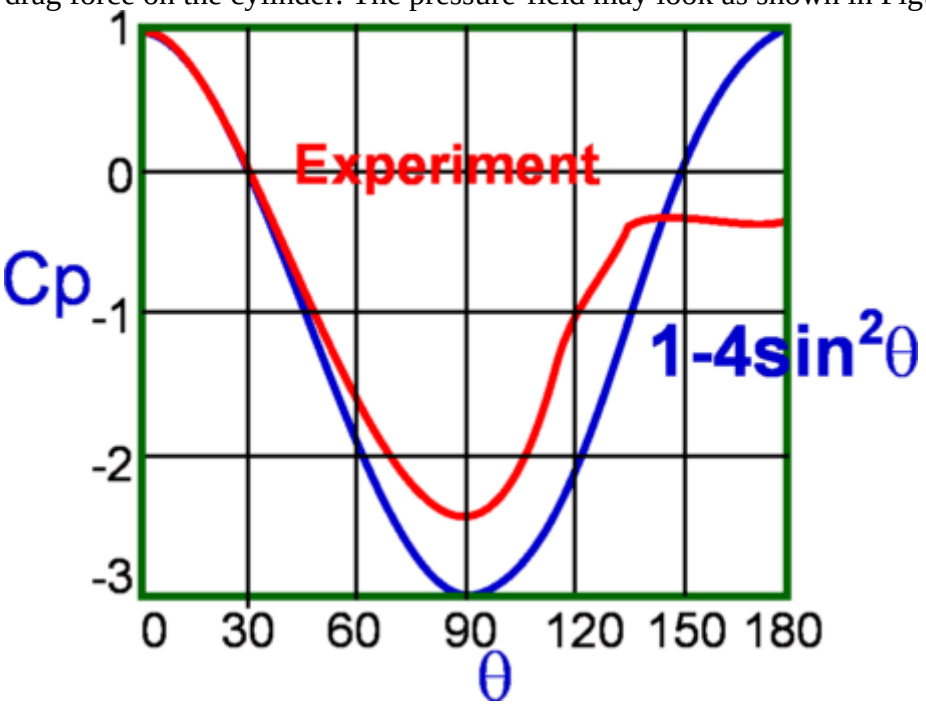

Figure 4 Pressure-field to cylinder surface by flow around it. Positive value means pressure into the cylinder while negative value means suction to the surface. The degree (DEG) is such that 0 degrees is fronting the current head on. (From MDP 2020).

Figure 5 shows pressure fields for different Reynolds numbers and hence different drag coefficients.

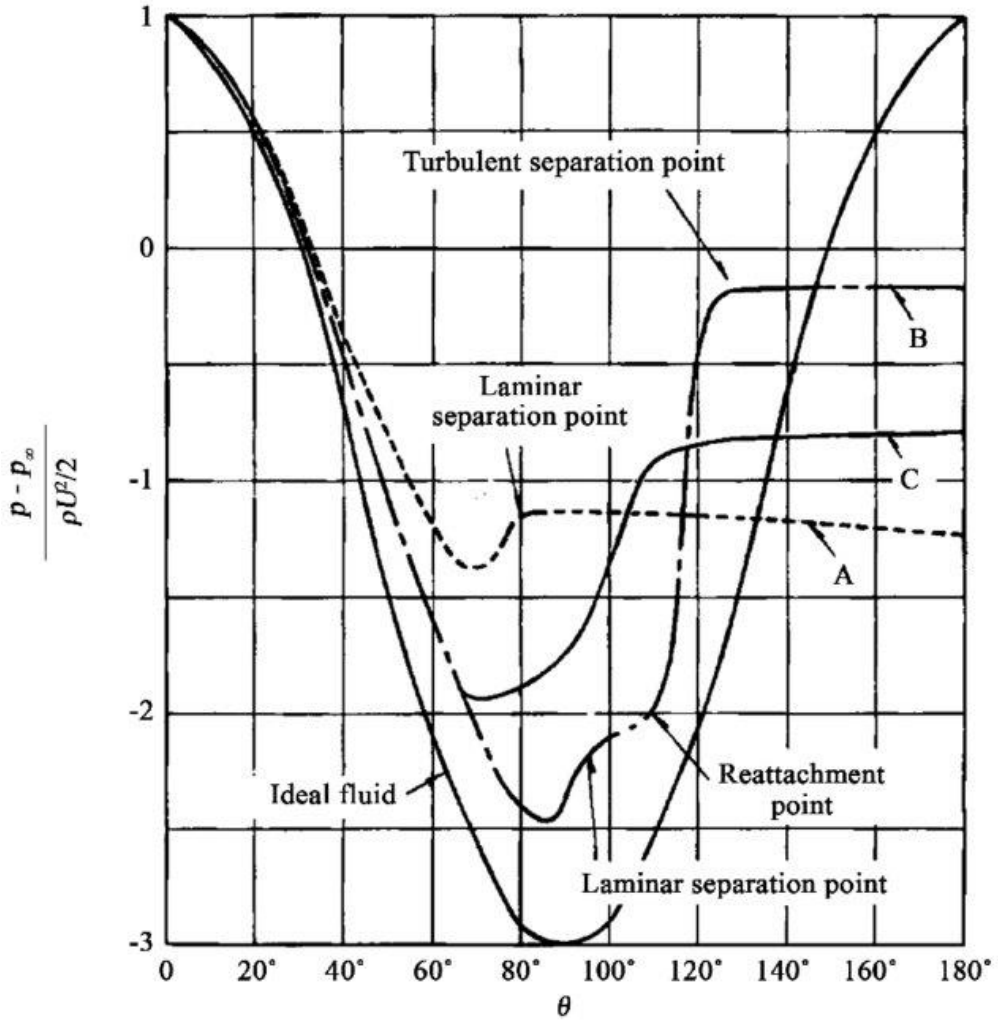

Figure 5 Pressure distribution as function of Reynolds number. (From Ogawa, S. and Kimura, Y. 2018).

The pressure field around a cylinder is implemented to AquaSim in a simplified way as shown in Figure 6. A drag and a lift coefficient is introduced. The pressure coefficient, C_p, upstream may be expressed as:

$$C_p = 1 - (C_l + 1)Sin^4\theta$$

Equation 4

For θ = 0 – 90 degrees. C_l is the lift coefficient given as input. Note that this corresponds to the analytical solution for an inviscid flow with C_l = 3.0. Then for the leeward side of the cylinder C_p is found as:

$$C_p = \min(1 - (C_l + 1)\,Sin^4(90 + (\theta - 90) * 1.5), -C_{wake})$$

Equation 5

Where C_{wake} is found by matching the overall drag to the cylinder, to the drag force derived from the input drag and lift coefficients.

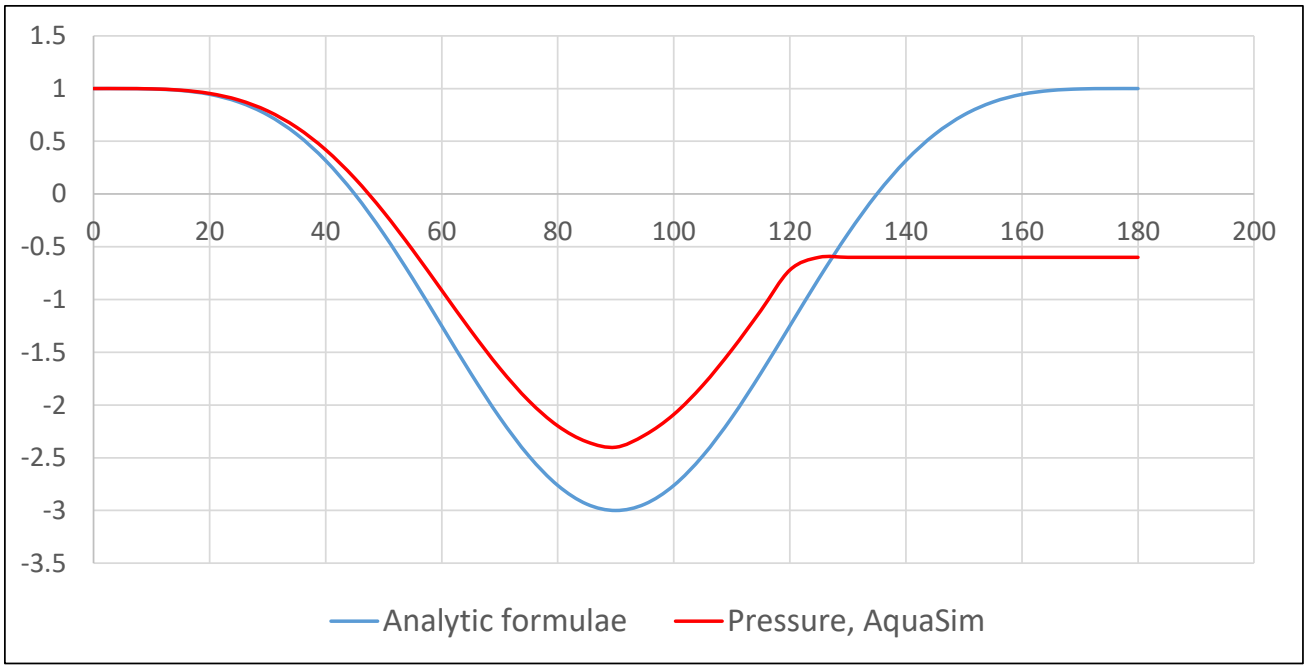

Figure 6 Pressure distribution around cylinder as calculated in AquaSim.

Having found the pressure coefficient, Cp, as a function of the angle between the element in the horizontal plane and the current flow, the force acting into a net panel with an area, A, is found as:

$$F_N = \frac{\rho A C_p}{2} {U_c}^2$$

Equation 6

The cross-flow principle is applied such that U_c is the part of the current velocity normal to the element at the element fronting the current direction. In addition, a skin friction force, F_s, can be applied and may be expressed as:

$$F_s = \frac{\rho A C_s}{2} U_{tan}^2$$

Where U_{tan} is the current flow acting tangential to the element, and C_s is the skin friction coefficient. The skin friction part of the force is applied for the current in the tangential direction. Both circumferential and along the length of the cylinder.

2.2.2. Effect of deformation of the cylinder

Figure 7 shows an impermeable net deformed by current. As seen, the front of the cylinder "flattens out" so that the drag coefficient for a cylinder seen in Figure 4 may be nonconservative comparing to a drag coefficient of 1.0 as given by the analytic formulae.

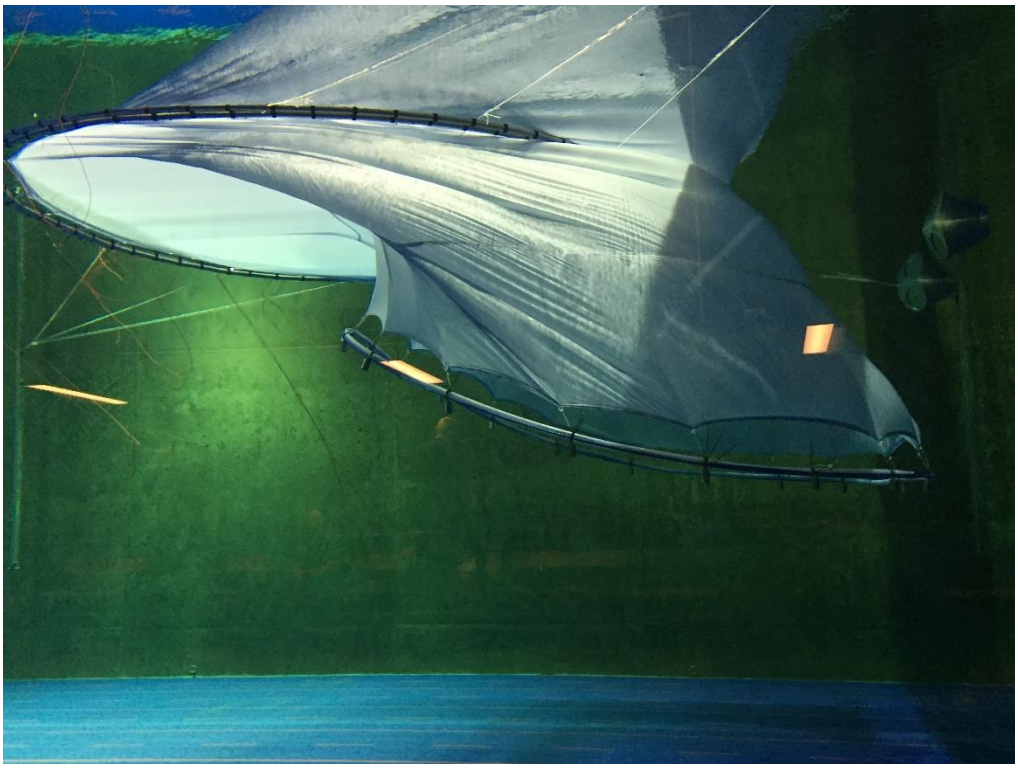

Figure 7 Deformed net (Egersund net 2020)

Hence, in AquaSim there is an option to introduce additional drag in the front part of the cylinder (For θ = 0 – 90 degrees.) applying an additional drag in this area, C_{add} as shown in Equation 7

$$C_p = 1 - (C_l + 1) Sin^4\theta + C_{add} \cos^4\theta$$

Equation 7

Note that the additional drag is not included in the calculation matching the drag and the pressure/wake. The pressure is increased according to Equation 7. This means that is a drag coefficient of 1 is used for the cylinder, and C_{add} is added, the total drag is hence higher.

2.3. Waves

Waves are a time dependent change in the water elevation and also the pressure in the fluid. The pressure below the water surface is in this case normally parted to the static part and the dynamic part of the pressure where the dynamic part of the pressure is a perturbation of the average hydrostatic pressure. Let the wave elevation be described by Airy waves (http://en.wikipedia.org/wiki/Airy_wave_theory). The water particles will then move in a circular pattern at infinite depth and an elliptic pattern in finite depth as shown in Figure 8.

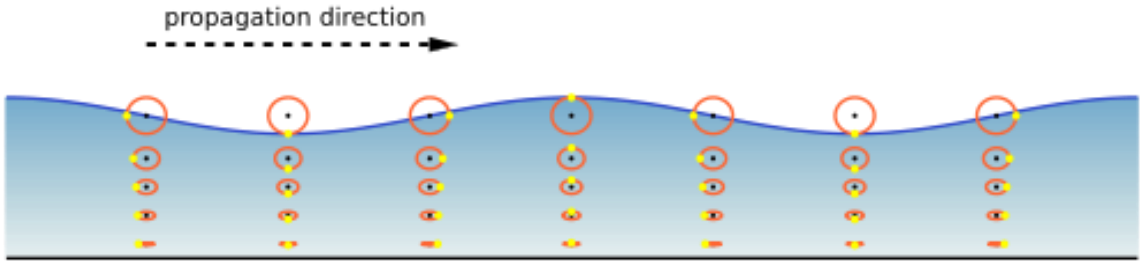

Figure 8 Velocity of water particles under propagating airy waves

Mathematically wave elevation according to Airy wave theory can be expressed as

$$\zeta = \zeta_a \, sin(\omega t - kx)$$

Equation 8

For a wave propagating along the positive *x*- axis.

Waves leads to a time dependent pressure component

$$p_d = \rho g \zeta_a e^{kz} \, sin(\omega t - kx)$$

Equation 9

where ρ is the density of the fluid. For infinite water depth and

$$p_d = \rho g \zeta_a \frac{cosh(z + h)}{cosh(kh)} sin(\omega t - kx)$$

Equation 10

for finite water depth. k is the wave number $k = \omega^2 / g$ for infinite depth and $k \tanh(kh) = \omega^2 / g$ for finite depth. Figure 9 shows pressure under a wave crest and how dynamic pressure and static pressure distributes under a wave crest.

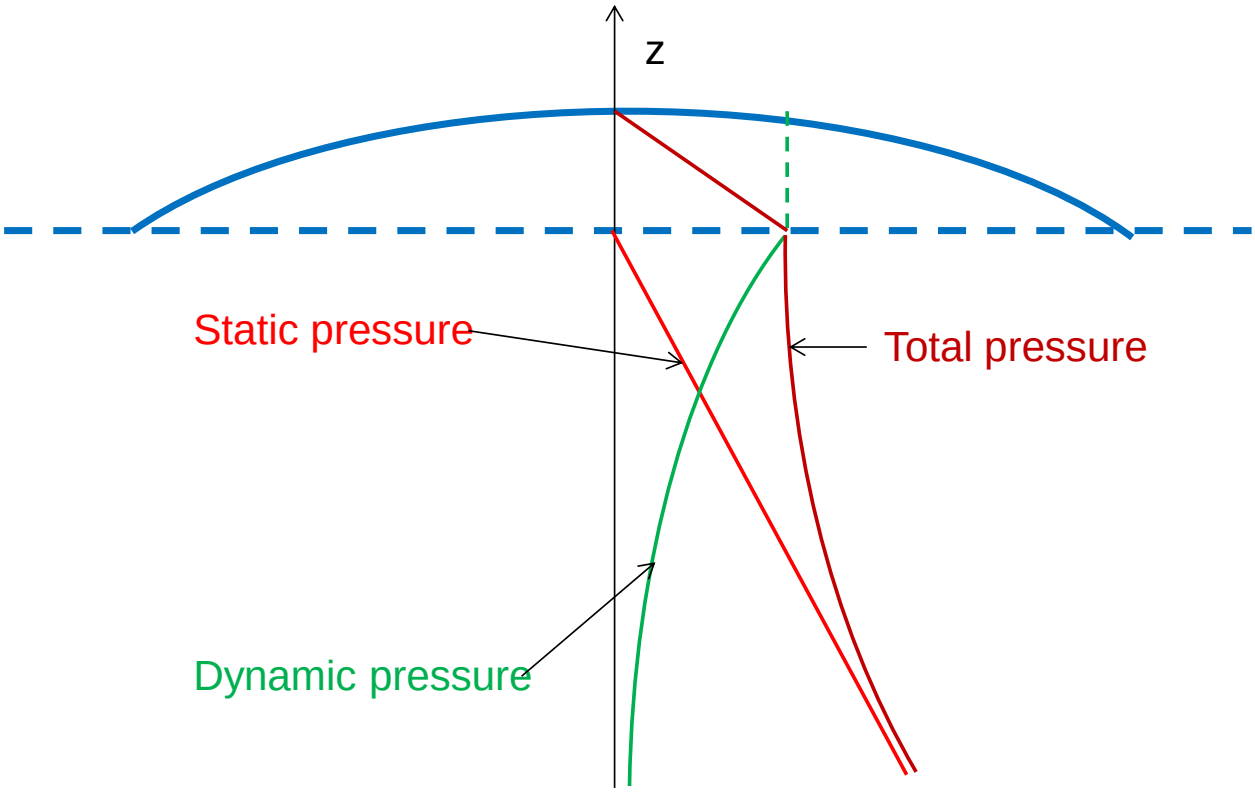

Figure 9 Sea pressure under waves

As seen from Figure 9 the total pressure is the static pressure plus dynamic pressure and can be formulated as:

$$p = p_d - \rho g z + p_{atm}$$

Equation 11

Simplified this can be viewed as the hydrostatic pressure under the wave crest, but with the effect of the wave decaying with depth. In the area above the mean water line and under the wave crest, the pressure is calculated simply as the hydrostatic pressure under the instant wave crest. Figure 10 shows the pressure distribution under a wave through. The static pressure is added to the dynamic pressure, and if the total pressure is less than 0, the surface is out of water and the dynamic pressure is set to the negative of the static pressure so that the total pressure is 0.

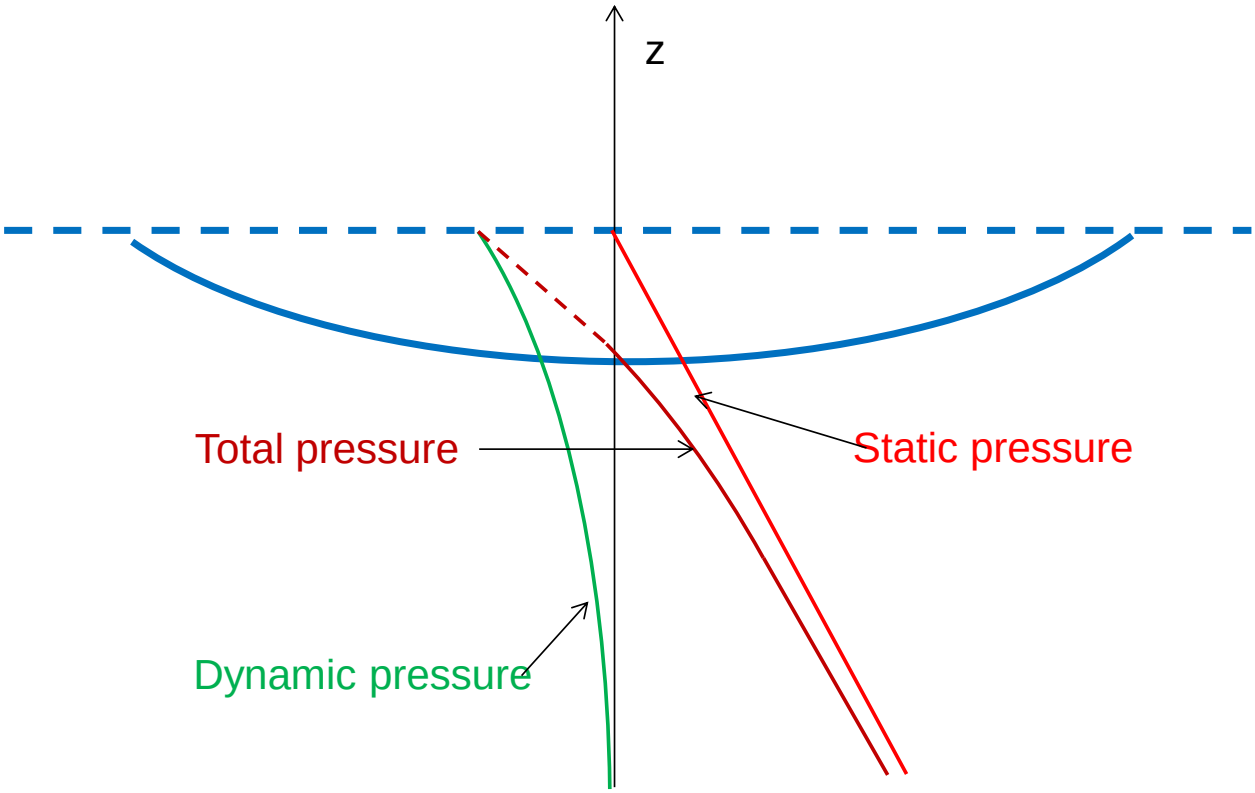

Figure 10 Pressure under wave through

Consider a body submerged in water under waves

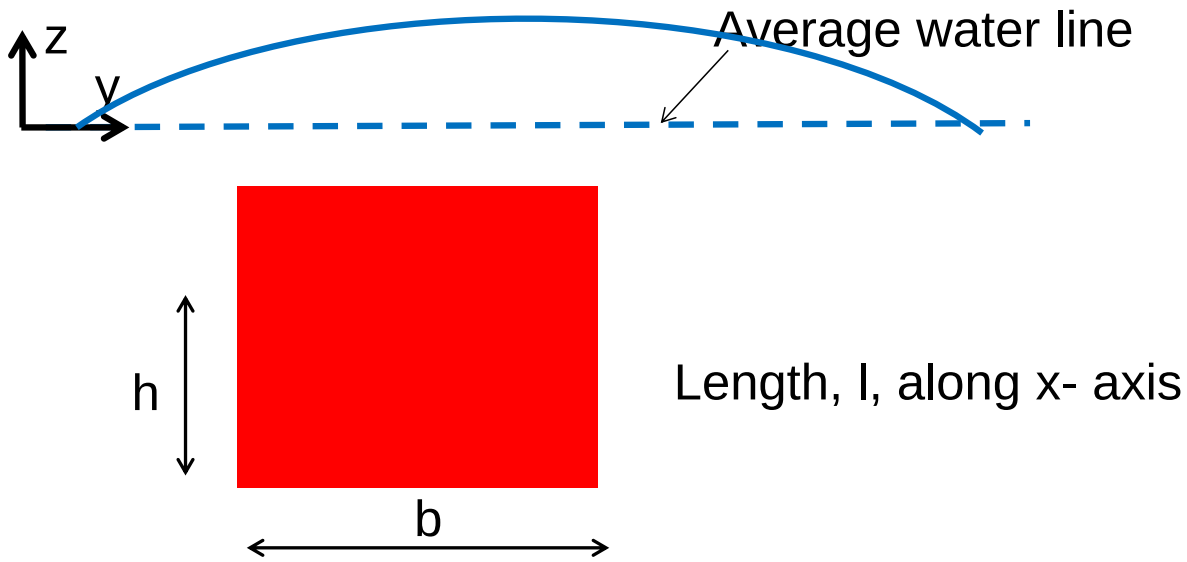

Figure 11 Submerged body

2.3.1. Hydrodynamic forces to a stiff body

Hydrodynamic forces are forces originating from waves and can be considered a pertubation to the hydrostatic forces. In this section current is neglected. Current influence the total water pattern and hence forces. So do viscous effects which also are neglected in the wave diffraction theory presented in this section.

For practical purposes the hydrodynamic forces are subdivided into nto a Froude-Krylov term and a diffraction term, were the Froude-Krylov term is force due to the undisturbed pressure field, and the diffraction term is force due to that the object/body changes/disturbes this pressure field.

The boundary conditions for being solved are such that the Froude Krylov and the diffracted waves summed satisfy the applicable boundary condition to the body.

Then waves and pressure field caused by body motion is derived and introduced as damping and added mass.

2.3.1.1. Froude Krylov force

Forces from water to a submerged body will be integral of the pressure around the body. As the static pressure is constant, we may integrate the pressure to find the force on the body. We start out with integrating the pressure over the surface, then the Froude Krylov force, F_{FK} is

$$\vec{F}_{FK} = -\iint_{Sw} p\vec{n}ds$$

Equation 12

Where p is the pressure introduced by the undisturbed wave field,

2.3.1.2. Diffraction force

The pressure under the waves is associated with fluid velocity. This means that to keep its position, the body in water will introduce a change in the fluid particle motion on and around the body. For a fixed body, the fluid velocity must be zero normal fluid velocity to the body as shown in Figure 12. The forces caused by the pressure of the undisturbed incident waves are called the Froude Krylov forces. The presence of the body is disturbing the incident waves. The These forces caused by the body´s disturbance of the wave field is called "diffraction forces" and is denoted F_D. The normal velocity to the body for the diffracted wave field is at any time opposite to the velocity caused by the incident wave.

Diffraction forces are calculated either by the MacCamy Fuchs (1954) analytical solution or numerically.

MacCamy Fuchs theory is appropriate for vertical cylinders in water where it gives an analytic estimate for the forces acting under the assumption the validity of the method. Application of this to impermeable nets have been outlined in Berstad and Heimstad (2015).

The numerical calculation for derivation of diffraction forces are based on "sink-source" analysis. This means that the object is subdivided to flat plates where there is a source located at each plate. The numerical boundary condition is that this source "blows out" exactly the same amount of water in the opposite direction to counter the water transport through the plate estimated by the Froude Krylov wave theory. This makes it such that the total fluid velocity normal to the plate is 0. For details se e.g Babarit and Delhommeau (2015)

In AquaSim the panels align with the element panels being impermeable nets of shell elements.

The pros for using numerical calculation of the diffraction forces is that it can cover general geometry. The cons are that there are a large amount of numerical issues that can occur for the numerical calculations. Hence it is of large importance to verify the response parameters seen in AquaView to check the validity of the estimated response.

To describe one such possible origin for numerical issues is that in the analysis a sink-source is blowing water also to the inside of the body, and if the period is close to e.g. sloshing

period this can give singularities/resonance effects in the solution making the results unphysical and invalid.

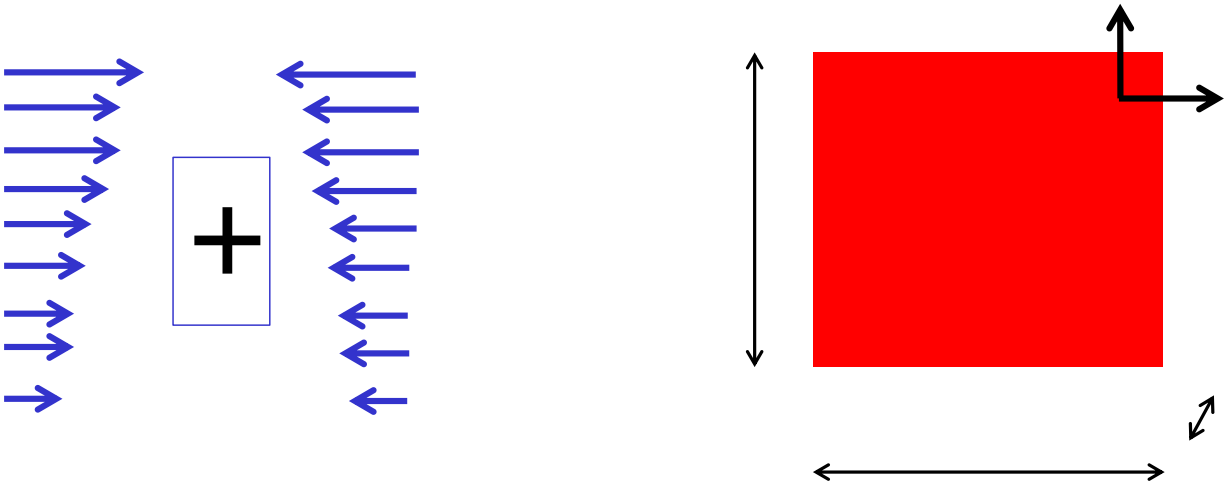

Figure 12 Velocity field around a submerged body

$$\vec{F}_D = -\iint_{Sw} p_D \vec{n} ds$$

Equation 13

The total force to the body is then

$$\vec{F} = \vec{F}_{FK} + \vec{F}_D$$

Equation 14

2.3.1.3. The splash-zone

In the splash zone, it is kept track of the total pressure for both hydrostatics and hydrodynamics such that it the total pressure (see Figure 10) is negative, the pressure is set to zero. This is one of the components causing wave drift forces, and this part of drift forces will occur also in case drift forces are not ticked off in the AquaEdit.

2.3.1.4. Wave drift forces

The nonliearity that arises from the in and out of water is one of the 2nd order effects that give rise to drift forces. An overview of this and handling in AquaSim is found in Aquastructures (2013b). Note that for impermeable net elements and shell elements where the load application described in this section is applicable, waves caused by body motions are not included in the wave elevation causing drifting. That means the drift forces will be underpredicted for cases where this is important.

The reason this is not included is that contrary to stiff objects being modelled, the objects modeles in Aquasim are “soft” objects where the velocity and acceleration can be different for different parts. This also means that the diffraction theory may not be a good predictor for loads. The more flexible the response is the less diffraction there will be. This must be carefully evaluated by the engineer.

2.4. Hydrodynamic forces to a flexible panel

Consider a fully flexible body following the particle motions associated by waves. Consider this applied to a part of a mesh where the waver on the outside of the mesh is assumed to follow the pressure distribution in wave according to linear wave theory. Assuming that in the calculation it is calculated dynamic pressure to one side of a panel and assume a solution where the panel is assumed to follow the flow motion perfectly. This will be like a “free tarp” in water.

In an analysis where the load is distributed to one of the sides of the panel, The load to the panel will according to airy wave theory for deep waves be

$$\vec{F}_{FC} = \rho g \zeta_a e^{kz} \sin(\omega t - kx) \;\; \vec{n} A$$

Equation 15

Where $\vec{n}$ is e vector normal to the plane of the mesh plate. And A is the area of the plate. Let’s assume that this is the load applied in an analysis program and that we would like to derive a response where the panel follows the particle motions of the wave like a “free tarp”. As this is a harmonic motion, the dynamic response equation is applying such that the response can be derived by the harmonic equation

$$F = ku + c\dot{u} + m\ddot{u}$$

Equation 16

The velocity of the incident wave, the wave elevation is

$$\zeta = \zeta_a \sin(\omega t - kx)$$

Equation 17

And the horizontal part of the velocity is

$$\dot{u}_{xw} = \zeta_a \omega e^{kz} \sin(\omega t - kx)$$

Equation 18

Hence a solution

$$c = \rho g / \omega$$

Equation 19

Will satisfy lead to horizontal motion along with the particle motion of the plate, given the panel is perpendicular to the wave direction. This means that for a “free tarp” with a vertical side where the waves approach normal to the side, introducing Equation 19 as a damping term

will lead to a response motion where the tarp follows the horizontal motions of the wave particles.

For the vertical motion,

$$u_z = \zeta_a e^{kz} \sin(\omega t - kx)$$

Equation 20

$$k = \rho g$$

Equation 21

will lead to a possible solution. This is added as stiffness in the vertical direction. It is not good to base a solution on stiffness since there is no related work, hence, consider the velocity that will be

$$\dot{u}_z = \zeta_a e^{kz} \omega \cos(\omega t - kx)$$

Equation 22

Meaning that for the solution in Equation 19 to be applicable, a force corresponding to the Froude Krylov forve Equation 15 must be set to Equation 23 instead.

$$F_3 = \rho g \zeta_a e^{kz} \cos(\omega t - kx)\, A_z$$

Equation 23

As an option, damping in the vertical direction can be chosen to be different that in the horizontal direction, but 1 is consistent with a tarp following the water particle motion in the direction normal to the plane.

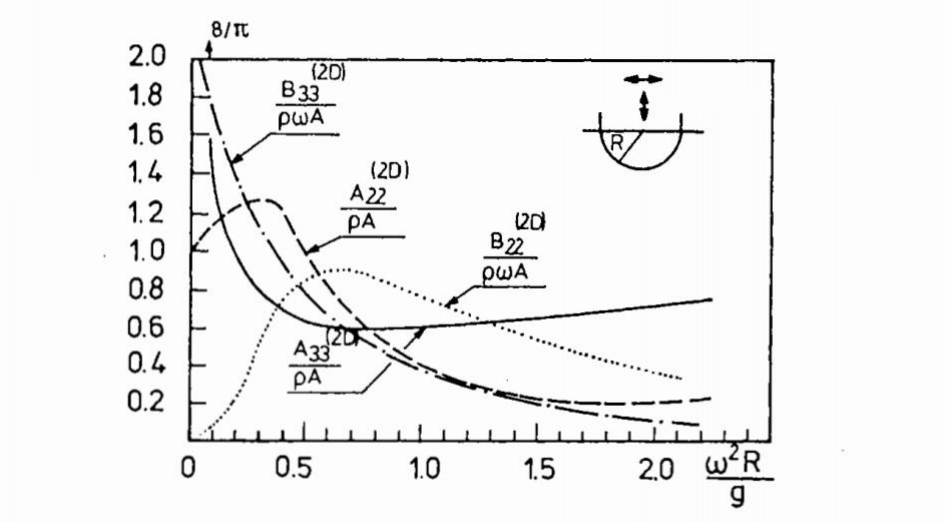

Fig. 3.6. Two-dimensional added mass and damping in heave and sway for circular cylinder with axis in the mean free-surface. Infinite water depth. ($A_{22}^{(2D)}$ = added mass in sway, $B_{22}^{(2D)}$ = damping in sway, $A_{33}^{(2D)}$ = added mass in heave, $B_{33}^{(2D)}$ = damping in heave, ρ = mass density of water, $A = 0.5\pi R^2$, ω = circular frequency of oscillation).

Figure 13 Added mass and damping for a cylinder in water (Faltinsen 1990)

In this solution (“the free tarp” load formulation) a vertical panes where the waves travels parallel to the tarp will have no pressure as response whereas the pressure is interpolated based in the projected frontal area for the range between. At the moment a normal pressure is applied, but that might be changed to just a force component in the wave directions depending on what fits best with empirical data as that is derived.

2.5. Added mass and damping

2.5.1. Hydrodynamic added mass and damping

The numerical solution from the hydrodynamic analysis also proposes added mass and damping from a distribution calculated numerically. Using coefficients of 1.0 means these parameters are used as proposed. They can be scaled by changing these parameters. The added mass and damping should be evaluated by the engineer.

When the MacCamy Fuchs formulation is applied, the added mass and hydrodynamic damping is based on coefficients relating to the radius of the element to the center point of the panels representing the object.

2.5.2. (Added) mass and Damping

Note that there are two ways to introduce both damping and “mass” cause by water being accelerated such that it acts as added damping. For the mass part the water outside the tank can be the hydrodynamic added mass and the water inside that tank can be the (added) mass. However, AquaSim only cares about this mass which is summed and added normal to the surface only. Note that for the water inside the tank it is possible to model such that all inside mass is accounted for with respect to weigh, but only parts of is to follow the harmonic motion on the period.

With respect to damping, it can be introduced both through hydrodynamic damping or damping according to Equation 18. These are added for the total damping. In addition, Rayleigh damping and damping in the Newmark Beta methodology are damping that may be introduced. The end user must keep track of the total damping compared with knowledge of how large the damping should be.

2.6. Wave drift forces

When drift is turned on, also the pressure caused by the velocity term of the Bernoulli equation is accounted for (see e.g. Aquastructures 2016). The wave drift effect caused by the in and out of water is accounted for under all conditions.

Note that in the consideration for the wave drift forces waves caused by oscillation of the body is not accounted for. This is because in the analysis bodies are described by many nodes and are in general flexible so that “stiff body motion” is not a valid expression. This means that engineers must evaluate this carefully.

2.7. Hybrid load model

The hybrid load model is an option to used which can be applicable for cases between the cases og stiff structure and flexible systems. When the hybrid solution is used, loads are based on one part from the flexible tarp formulation and the other part from the MacCamy Fuchs (MF) or numerical diffraction (NUM) solution. The user decide how much each part accounts for. If as an example scaled factor is 0.3, 30% of the loads are based on the MF og NUM model while 70 % of the loads are calculated from the free tarp formulation in Section 2.4

2.8. In and out of the waterline

At each timestep, the waterline is kept track of, including the wave elevation corresponding to the pressure from the diffracted wave. At each time instant, total pressure consisting of the pressure caused by waves and the hydrostatic pressure is calculated, and if this pressure is less than zero, the pressure is set to zero and the buoyancy is subtracted (as is only applied to tarp and not shell).

2.9. Waves and current combined

Combining waves and current, the following assumptions apply:

- Waves are assumed to "ride" on top of the current field.
- In case of varying current as function of depth, waves will ride on top of the current velocity at z = 0.
- For pressures originated by waves there are no adjustments due to current.
- When calculating the relative velocity to generate the pressure seen in Figure 6 in a dynamic state, the relative velocity is calculated at each element, or averaged in horizontal plane based on user choices.

3. CASE STUDIES

As set of case studies has been analyzed to check the validity of results.

3.1. Vertical cylinder, stiff

The Morisons equation reads:

$$F = \rho V\dot{u} + \rho C_a V\dot{u} - \rho C_a V\dot{v} + \frac{1}{2}\rho C_d A(u-v)|u-v|$$

Equation 24

Where C_a is the added mass coefficient and C_d is the drag coefficients which are parameters set empirically or analytically. Description can be seen at http://en.wikipedia.org/wiki/Morison%27s_equation The terms in Equation 24 are:

$\rho V\dot{u}$ is the Froude Krylov force. This term is added not only in the *z*- direction, for also in the horizontal plane.

$\rho C_a V\dot{u}$ is the diffraction force, i.e. related to the calculated diffraction of waves.

$\rho C_a V\dot{v}$ is the added mass.

$\frac{1}{2}\rho C_d A(u-v)|u-v|$ is the drag force.

V is the submerged volume and *A* is the area fronting the fluid motion. Set the viscous drag coefficient to 0, and consider a cylinder, can be written as:

$$F = \rho V\dot{u} + \rho C_a V\dot{u}$$

Equation 25

Where the first term is due to the Froud Krylov force and the latter term is due to the diffraction force. The analytic case says Ca = 1 meaning:

$$F = 2\rho V\dot{u}$$

Equation 26

The Morison Equation solution in Equation 26 should be found also in an analysis for a fixed object given that the velocity predicted by the incident wave in the centre of the object, $\dot{u}$. A test case with a cylinder as seen in Figure 14 has been established.

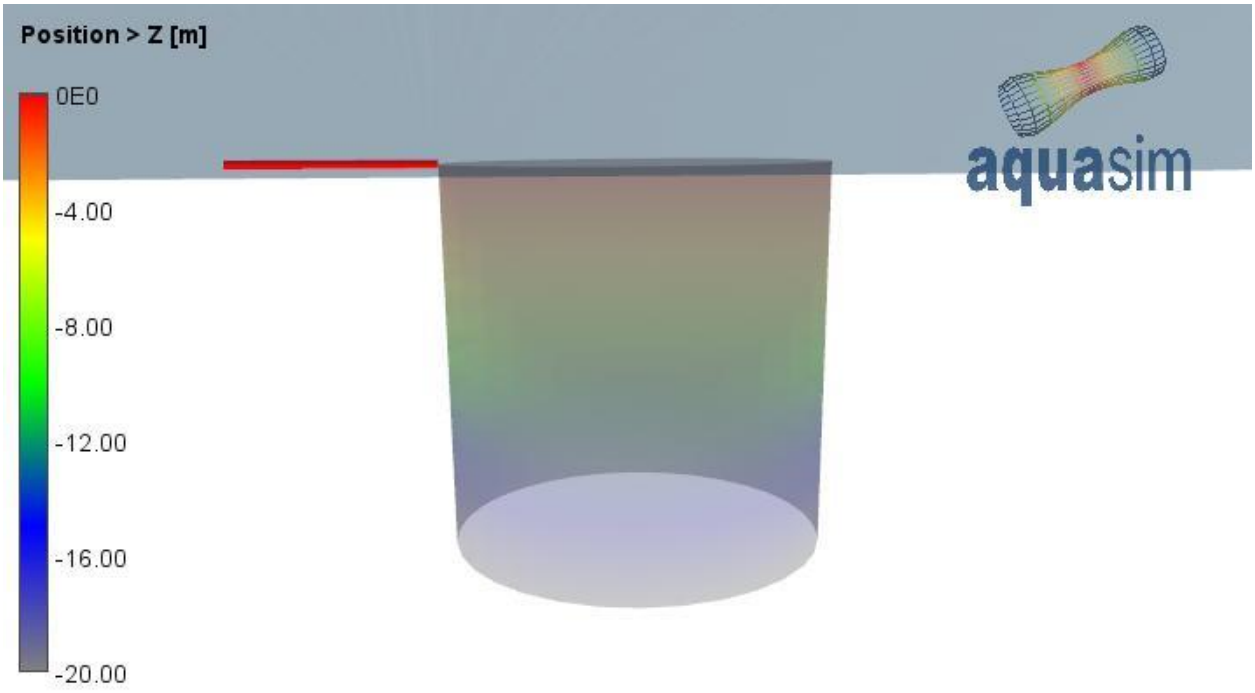

Figure 14 20 m deep cylinder with diameter 20 m. Depth of objects are indicated by colour. On top there is a truss element where which is fixed on the left

The cylinder in Figure 14 is withheld from motions except in the x-direction meaning that all forces in the wave direction must be distributed through the truss element. 320 elements/panels are distributed to the cylinder as seen in Figure 15. There are 32 panels along the circumference and 10 panels in the vertical direction. A refined analysis model has been established with 64 elements/panels along the circumference and 20 panels downwards.

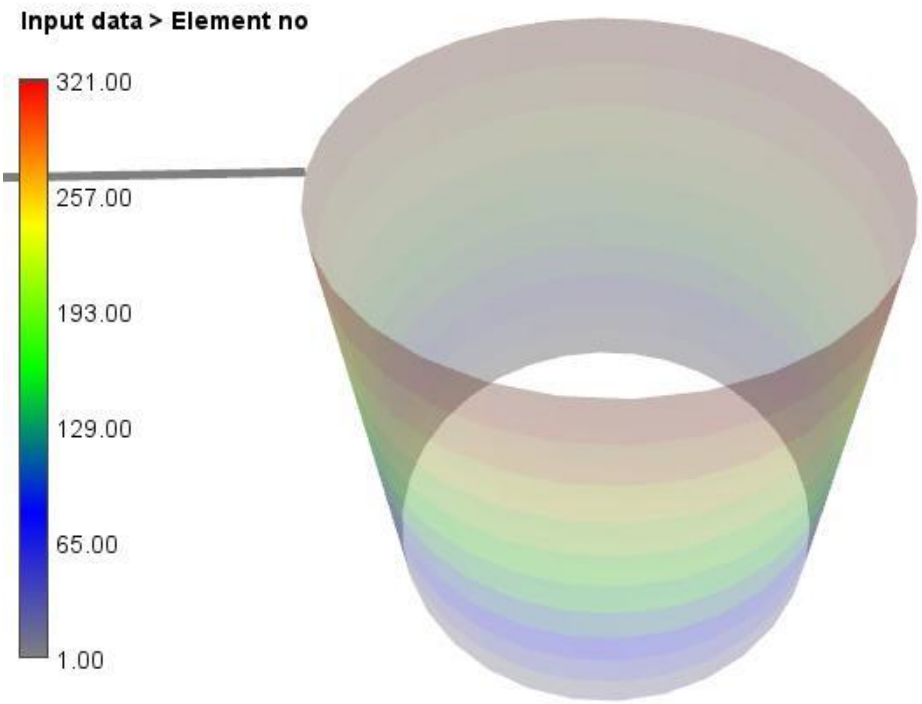

Figure 15 Elements and panels on cylinder.

Figure 16 shows results where the long wave theory is compared to results calculated by AquaSim using two different methods/models:

- AquaSim MacCamy Fuchs – In this case wave diffraction is calculated from the MacCamy Fuchs solution.
- AquaSim Numerical – In this case the numerical method is used to calculate diffraction.

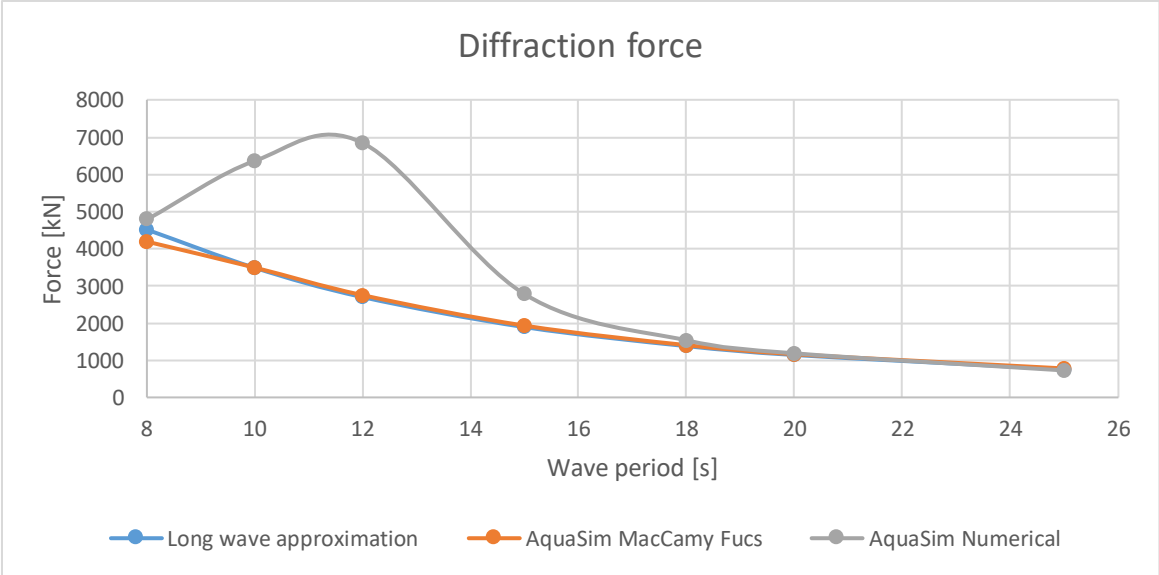

Figure 16 AquaSim results compared to long wave theory.

As seen, there is a good correspondence between the long wave theory and the MacCamy Fuchs analysis results. The results for the numerical analysis do not compare as well for some wave periods. In general aspect to be aware of considering numerical analysis:

- There might be errors in the numeric calculations.
- The theory may not reflect the modelled system.
- There might be resonance effects in the prediction. For instance, this could be a type of sloshing period. In this case there is a sloshing period for a shallow tank at period 12 sec. Since the tank is bottomless it can also be numerical effects from that as well.
- Diffracted wave may not have been found and is then set to zero.
- Since AquaSim is not interested in artificial results, the amplitude of diffracted waves larger than 1 is set to 1. This means that unphysical effects may be dampened. Hence the results should be evaluated, and load model carefully chosen based on such considerations.

AquaView have tools to evaluate certain response parameters. Parameters are seen in Figure 17.

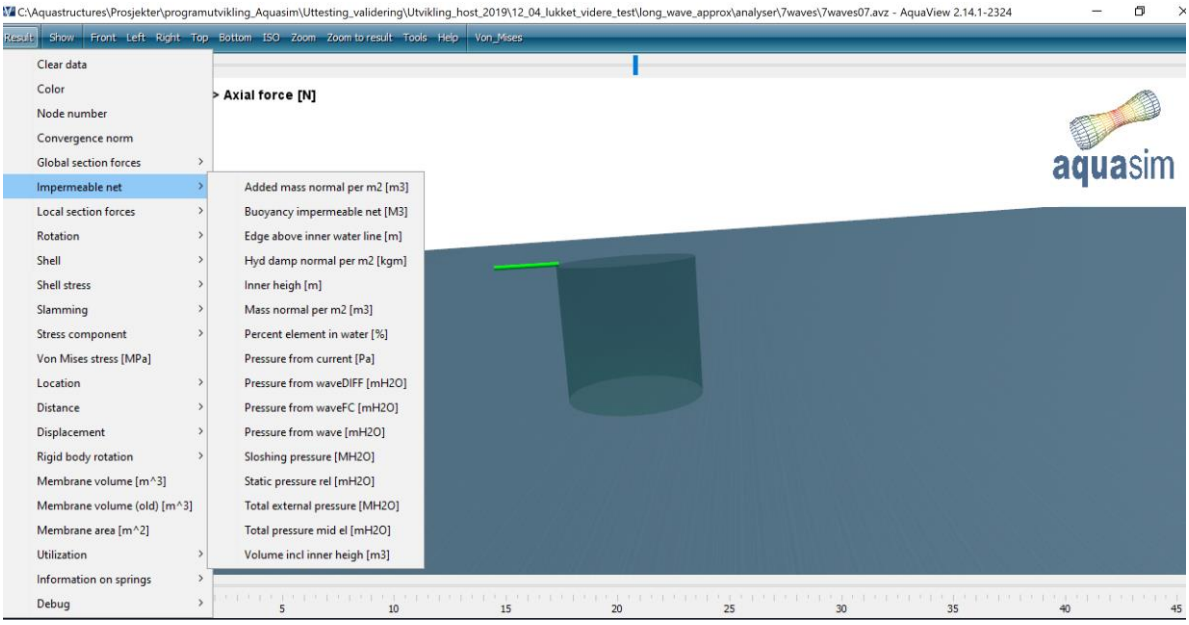

Figure 17 Response parameters impermeable net.

Note also that response parameters such as diffraction and added mass are based on the response from a stiff body. As discussed, this is not applicable for a fully flexible body, and for partly flexible bodies, the scaled diffraction option may be considered and is evaluated for a case in Section 3.3.

3.2. Case compared to reflection from a wall

Figure 18 shows a case with a wall, 5 meters thick and 20x20 wide and deep. For short wave lengths one may assume that the wave to a wall solution should correspond with analysis results.

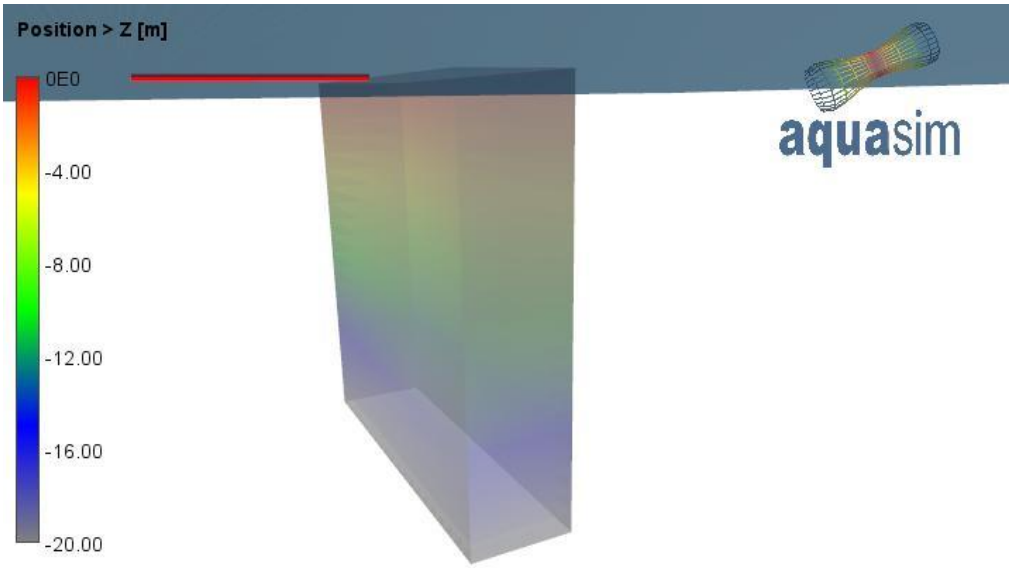

Figure 18 Test case 20x20 m wall 5 meter thick.

The model has 20x20 elements on each main side and elements 20 elements connecting the front and back sides and bottom as seen in Figure 19.

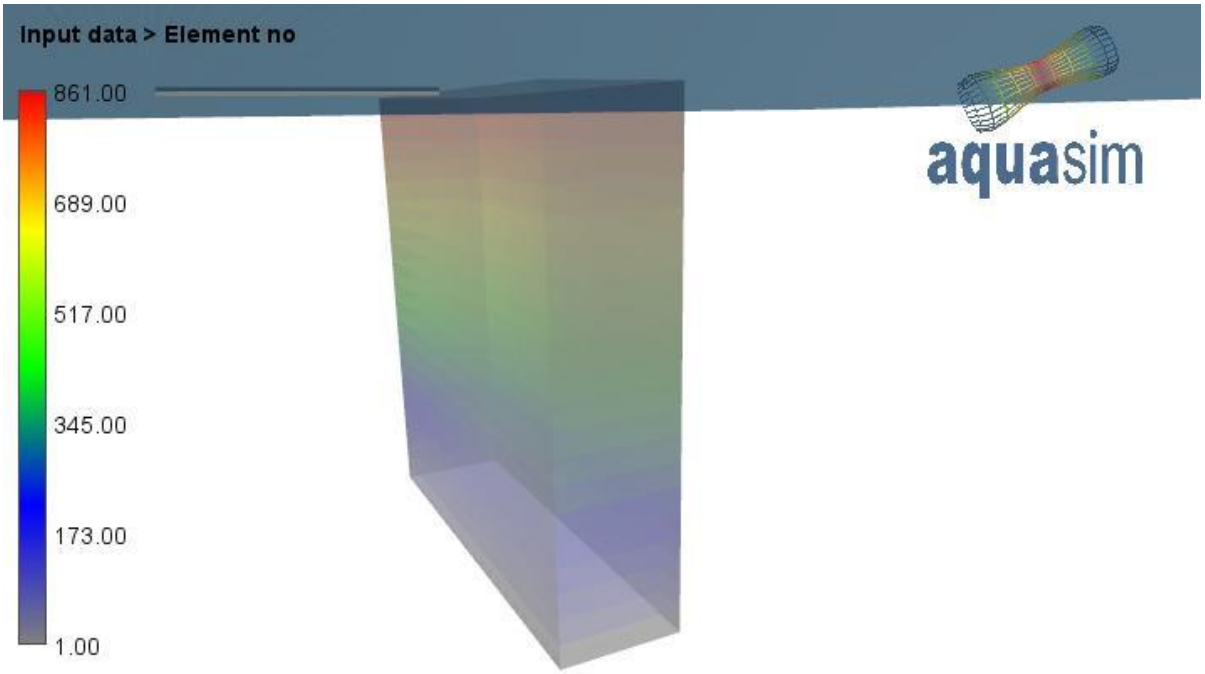

Figure 19 Elements in analysis model of square sections

The analysis model is only allowed to move along the x- axis and is withheld on the node to the left of the truss such that all forces will be seen in terms of axial force in the truss. Figure 20 shows results from AquaSim compared to an analytic solution based on the "standing wave" approximation. In this case only the numerical method is used in AquaSim.

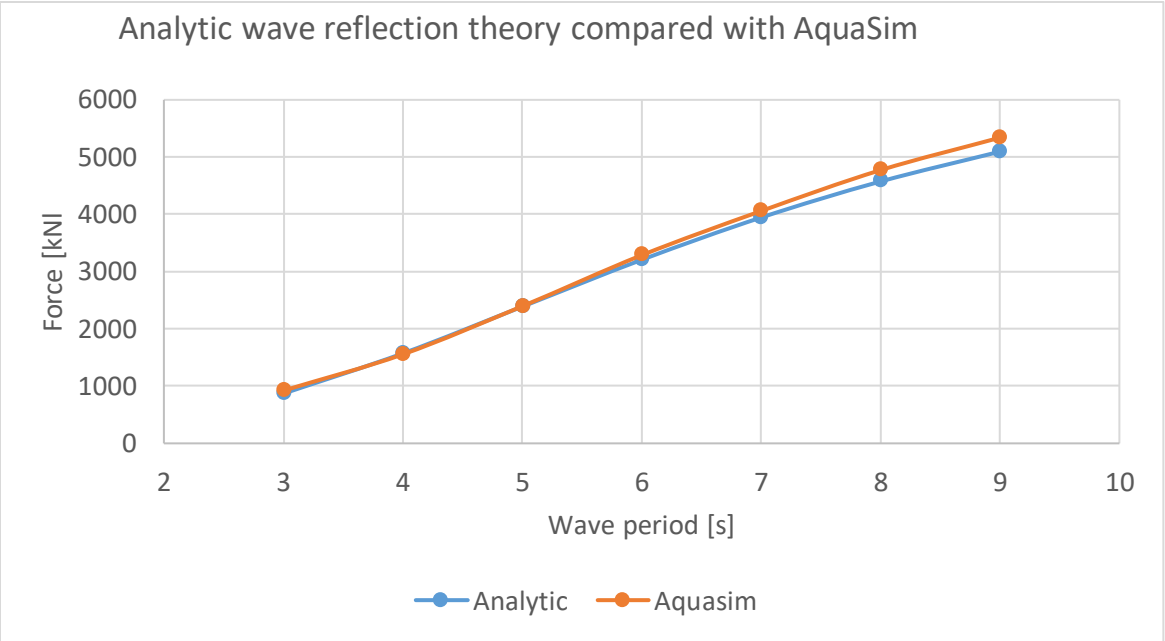

Figure 20 comparison of analytic formulae to numerical calculations

As seen from Figure 20 the results compare well for this case.

3.3. Flexible tube net

A flexible tube net as shown in Figure 7 has been analysed. The analysis model is shown in Figure 21.

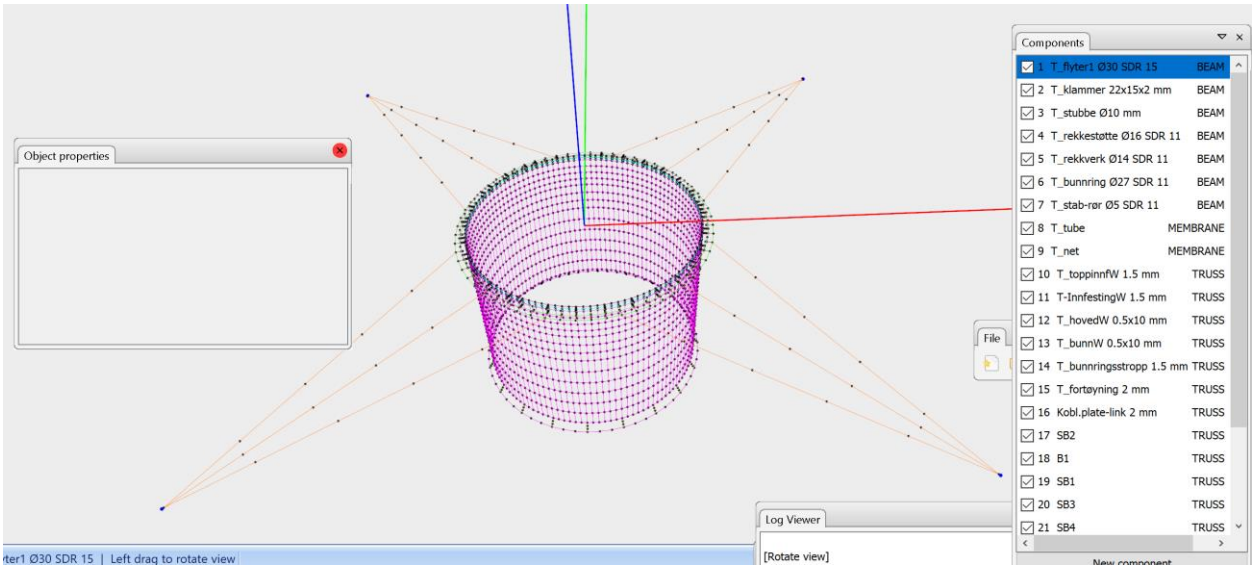

Figure 21 Analysis model Tubenet

Figure 22 shows the analysis model in model scale with the colours showing the vertical location. The coordinate system follows the AquaSim defaults with the z-axis pointing upwards and z = 0 is in the still water line.

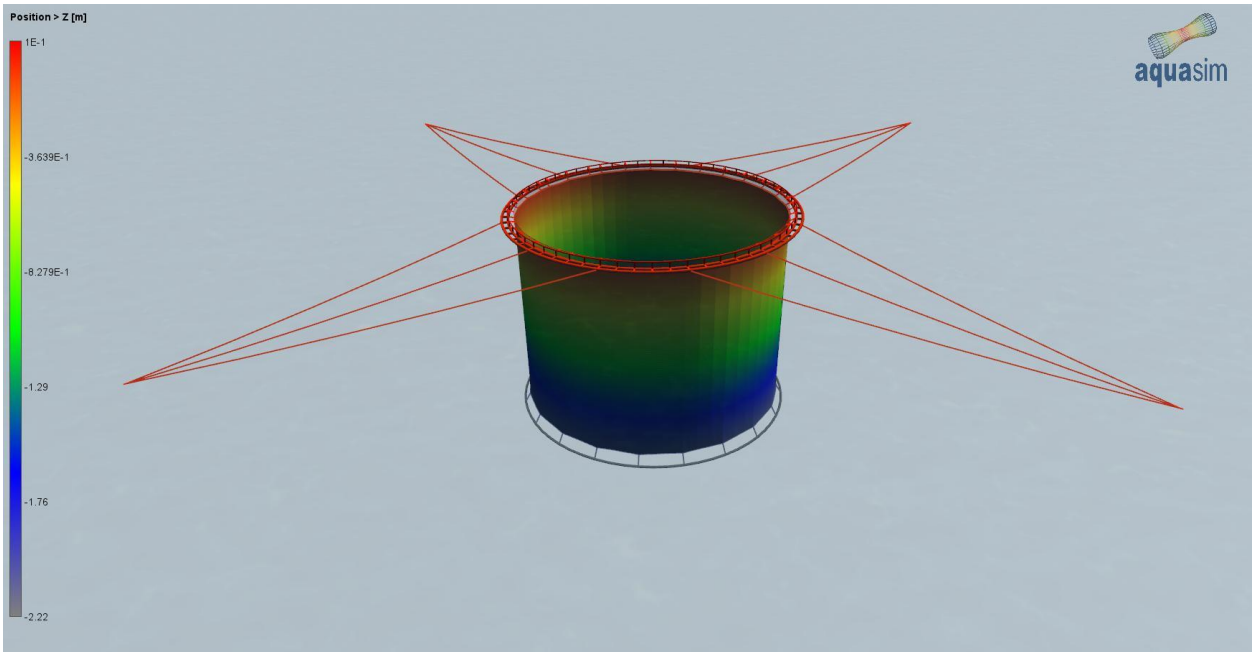

Figure 22 Tubenet. Colours shows vertical location in static equilibrium.

The bridles to the tubenet model has been are passed through one element as shown in Figure 23 and Figure 24 where loads have been measured.

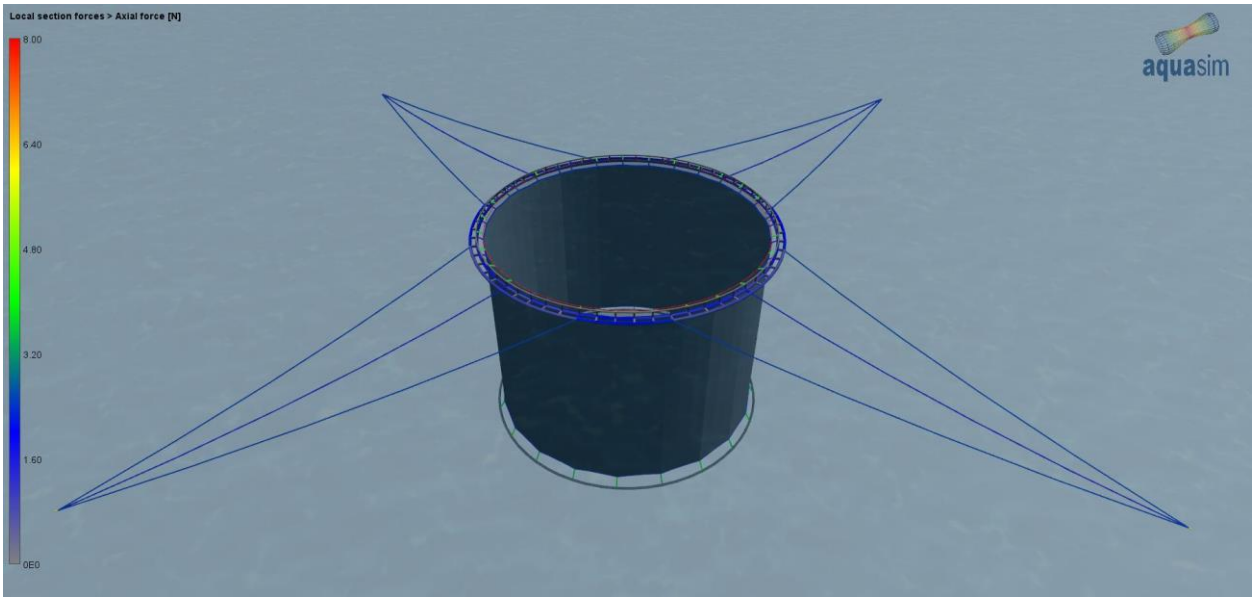

Figure 23 Local section forces in bridles in static equilibrium

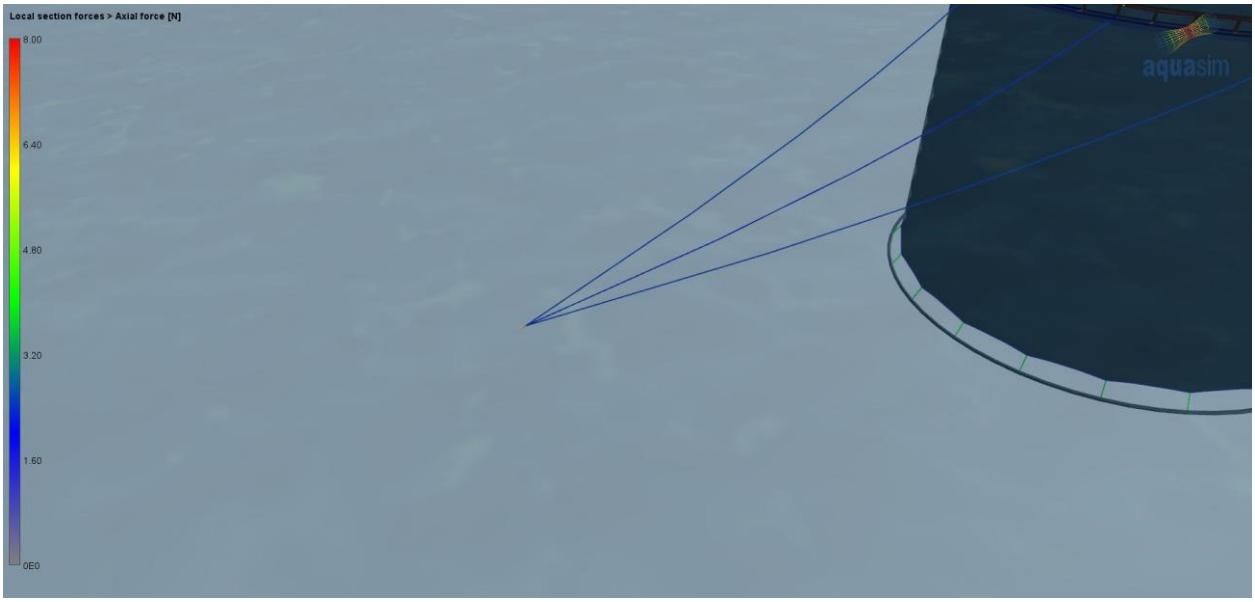

Figure 24 Bridles coupled through one endpiece which is the load cell in the model test. Forces from all bridles goes through the load cell both in the model test and in the analysis.

The analysis model is double symmetric. Figure 25 shows transverse (y-) location of the system. As seen from the figure, the model is 7 meters wide. The water depth of the tank is 2.7 meters and the width of the tank is 8 meters. Tank and effects from tank walls are not included in analysis.

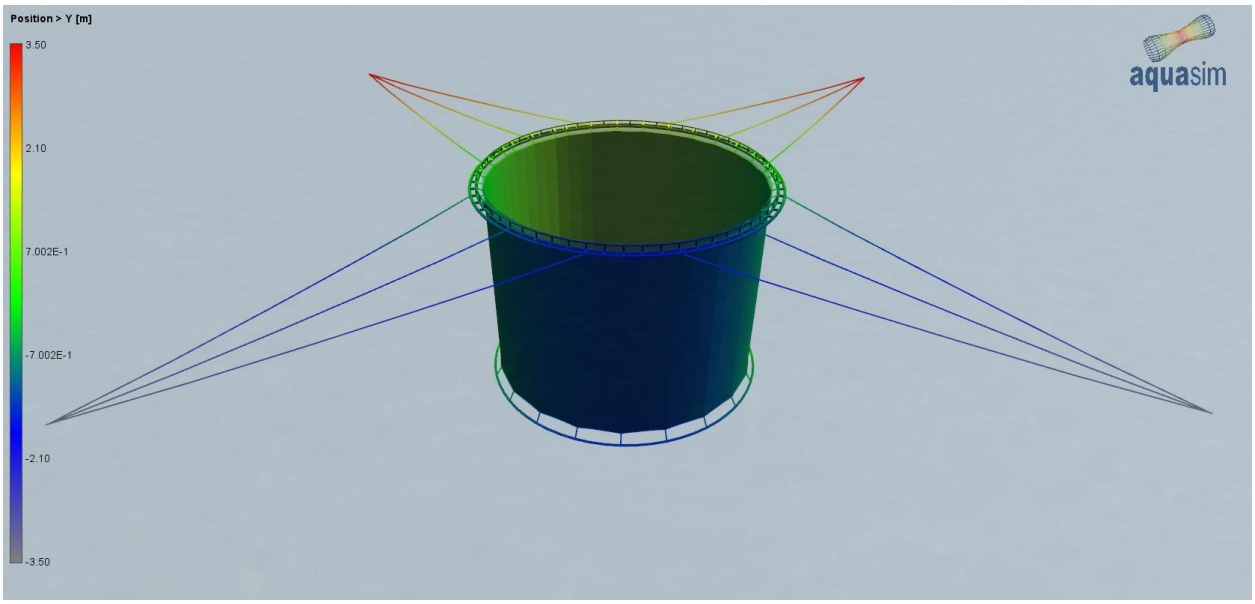

Figure 25 Transverse (y) position tube and bridles

3.3.1. Testing and comparison current

Figure 26 shows the tube exposed to 9.7 cm/s current, Figure 27 shows the same with 14.5 cm/s current and Figure 28 for 19.3 cm/s. Figure 29 shows the condition of 19.3 cm/s from a bird view.

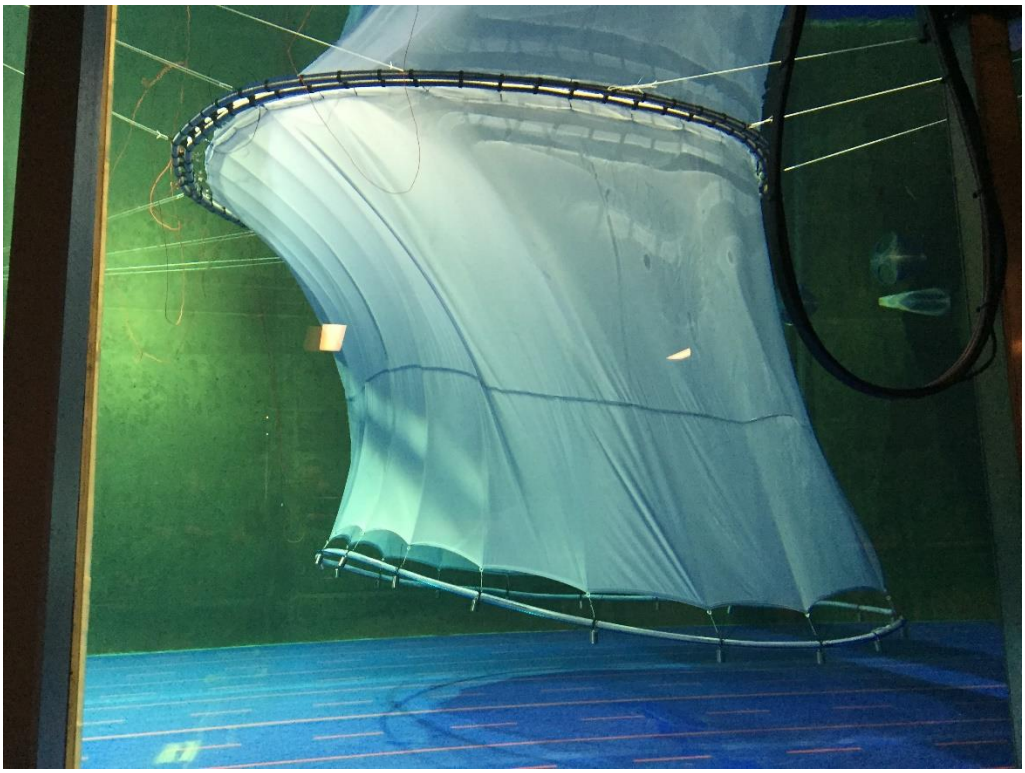

Figure 26 tube exposed to 9.7 cm/s current

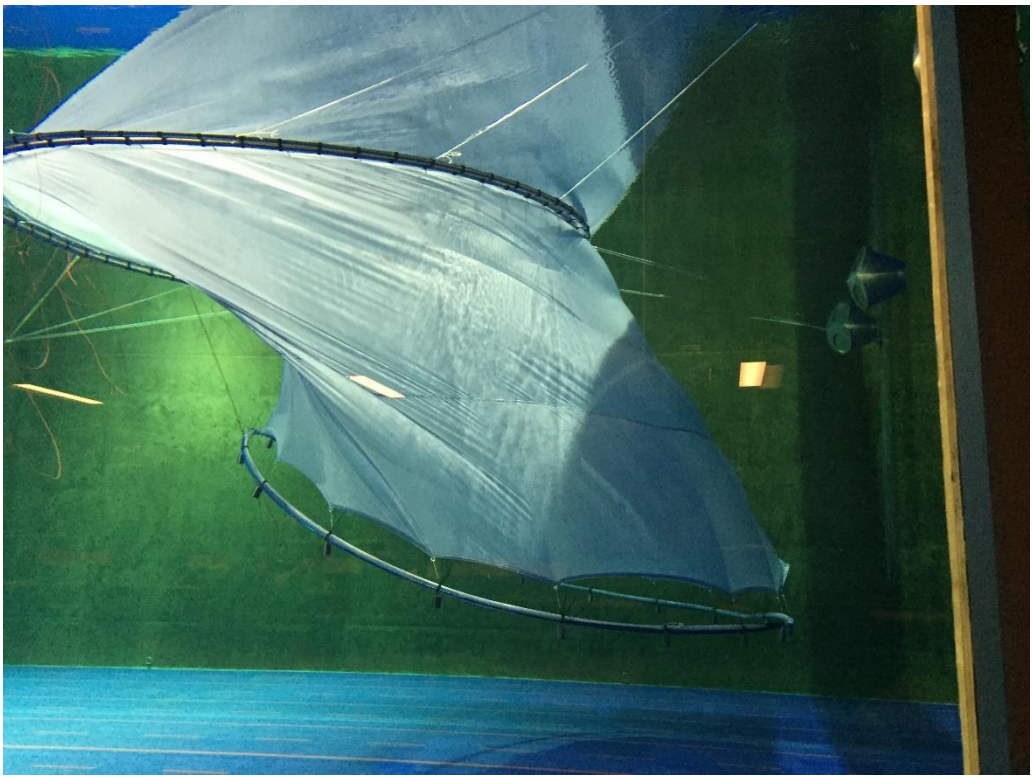

Figure 27 Tube exposed to 14.5 cm/s current

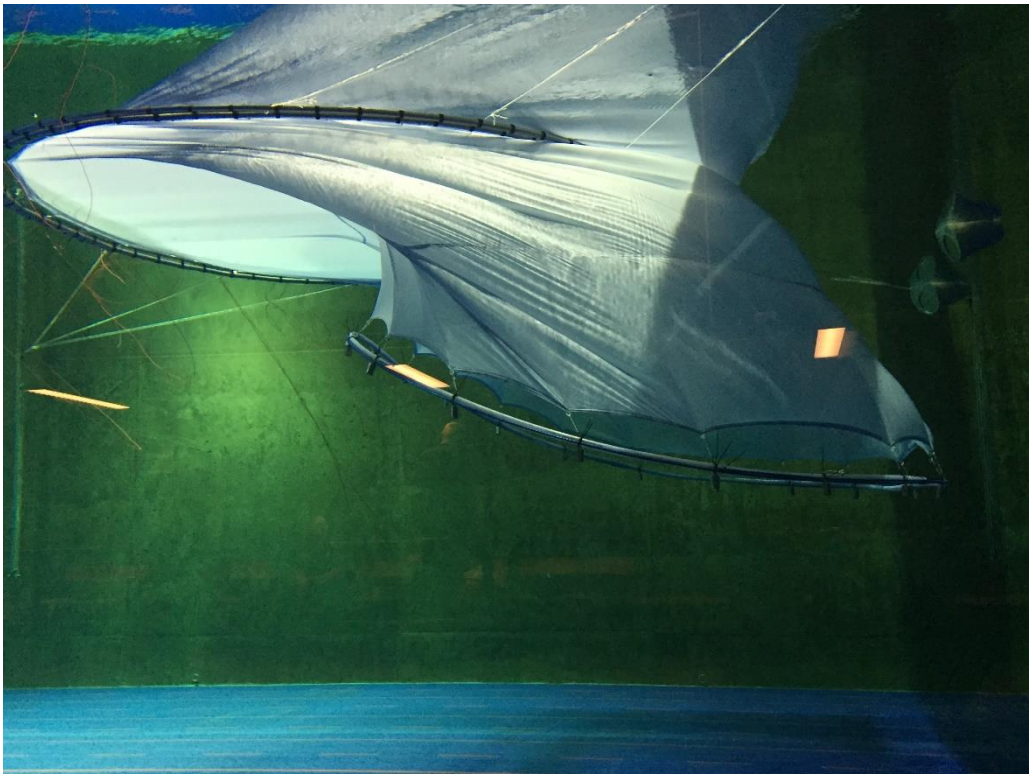

Figure 28 Tube exposed to 19.3 cm/s current

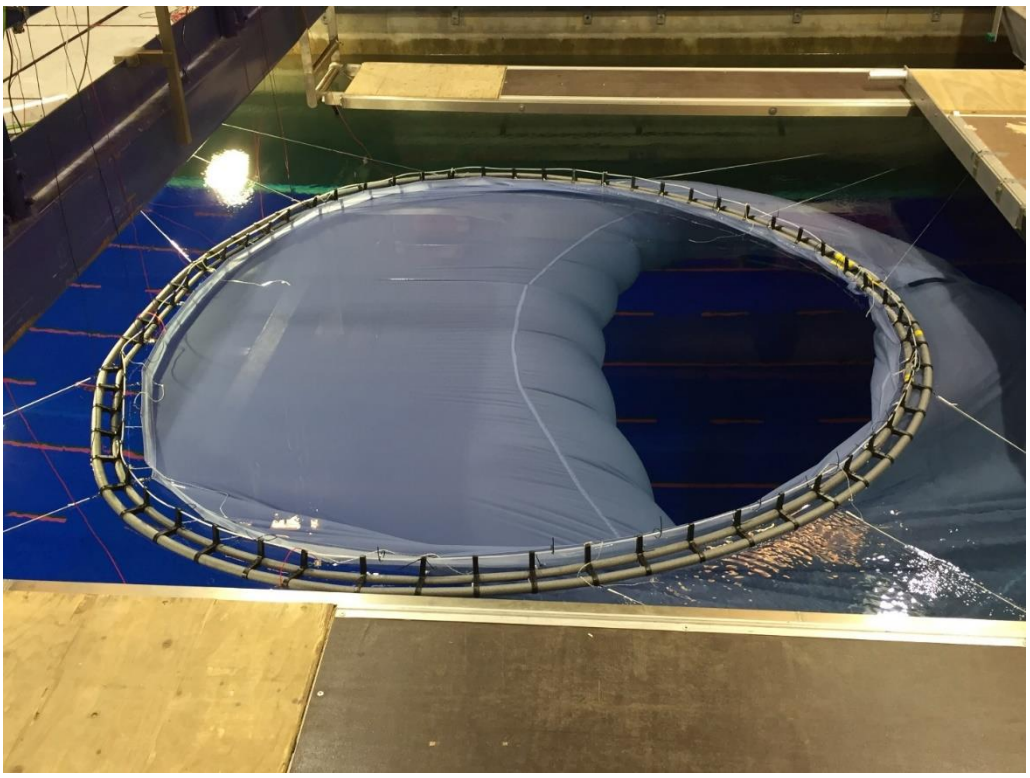

Figure 29 Tube exposed to 19.3 cm/s current bird view.

As seen from Figure 26- Figure 29, the tube deforms strongly, in particular from 14.5 cm/s current velocity. This means one can not assume the pressure around a cylinder to be the valid pressure formulation for the pressure-distribution and total drag. However, as the pressure distribution varies with the coefficients in the equations, and that the cross-flow method is part of the general formulation one can assume to be in the ballpark when comparing results.

Before comparing to analysis, the following should be noted:

- It is seen that the part of the tube upstream moves more upwards than the part downstream.
- The water tank has closed volume meaning the water pumped through the tank must pass through. As seen from Figure 26- Figure 29 in particular the bottom is close to the tube. The bottom ring of the tube is 2.2 m deep and the tank is 2.7 meters deep (SINTEF 2020). This may be of larger importance for 14.5 cm/s and 19.3 cm/s since as seen from Figure 26- Figure 29 the tube deforms such that most of the water seems to go under the tube and not around. For a node-formed net, the relation between the transverse area the flow is passing through where there is no net and the area where the tube is given in Table 1

Table 1 Transevese area of tank and tube.

Transverse area tank [m^2]	21.60
Transverse area tube [m^2]	6.05
Transverse free flow area [m^2]	15.55
Factor	1.39

As seen from Table 1 the water need to increase velocity by approximately 40 % to fulfil the continuous flow around or under the tank. As the tube deforms, the tube blocks a lower part of the transverse area, but in this case more flow is lead under the tank where the clearance is lower such that for comparing test and analysis. As an approximation, the results have been placed at two points where the first point is the nominal velocity and the second is the velocity multiplied with 1.2, half of the possible increase.

The load cells have been placed in each side of the upstream bridles as seen in Figure 30.

The load cells collect all the forces in the three bridles. Loads are symmetric between the bridles.

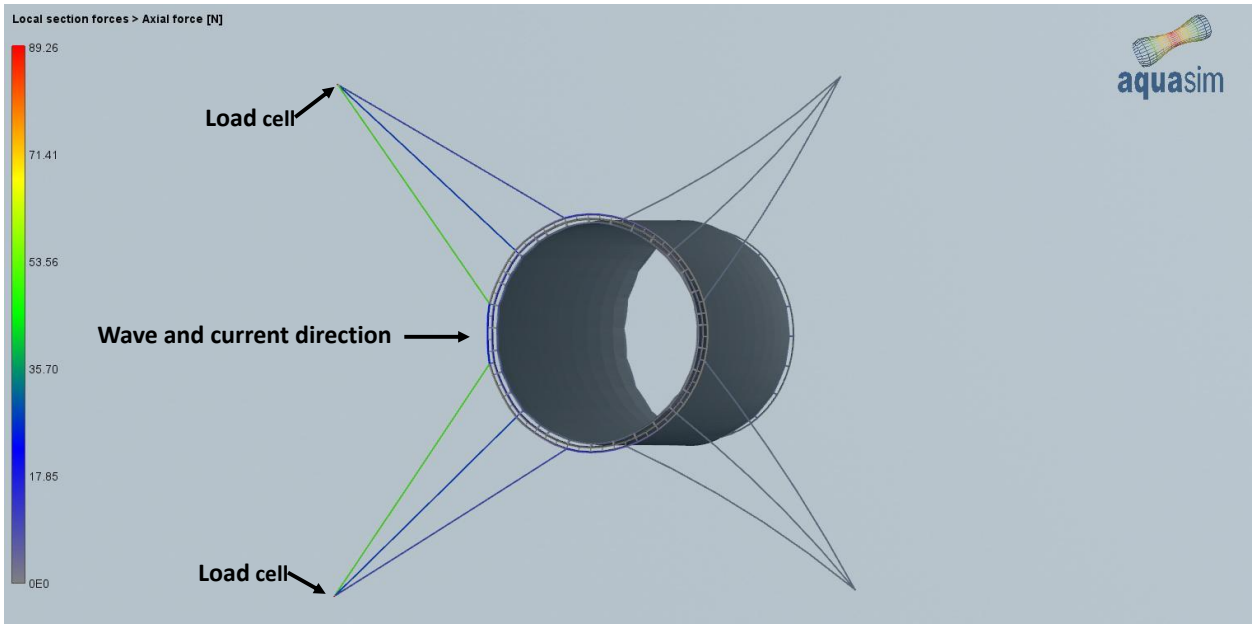

Figure 30 Location of load cells.

Figure 31 shown a comparison of results between model test and analysis. The following applies to this figure:

- The red lines represent measurements in the tank. The mark to the left of the test result at the nominal velocity while the right mark represents the a simplified upper bound by estimating how much the velocity needs to be increased with a factor of 1.2 due to the finite cross section in the transverse plane
- The results labelled “Test 1” is results from one of the load cells indicated in Figure 30 and “Test 2” is the other.
- The label “Max” is the maximum in the time series and “Mean” is the average value.
- MH2O is the unit “Meters of water” where 1 Bars = 10.1974 Metres of water.

The analysis has been carried out with the parameters given in Table 2.

Table 2

Lift coefficient	Cl	2.40
Tangential drag, friction	Ct	0.02

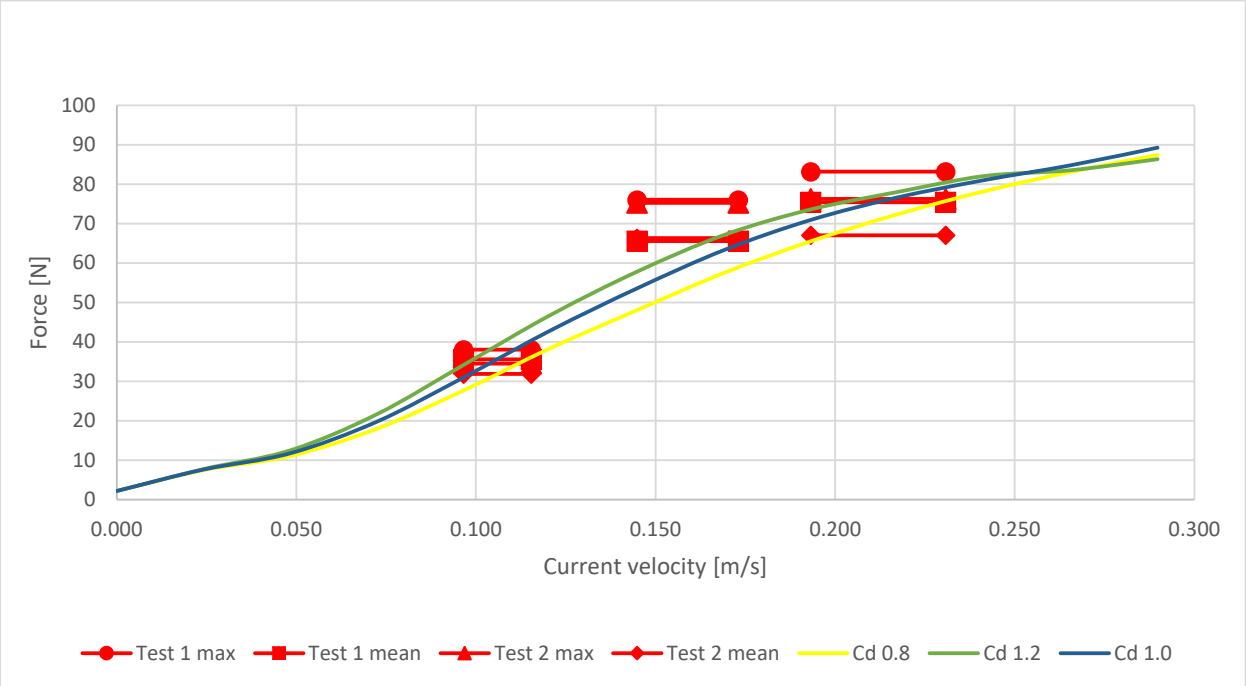

Figure 31 Analysis with a varying drag coefficient compared to test results (red)

Figure 32, Figure 34 and Figure 34 shows the response of the system with a drag coefficient of 0.8, 1.0 and 1.2, respectively. The right side shows a variation with extra drag in the front.

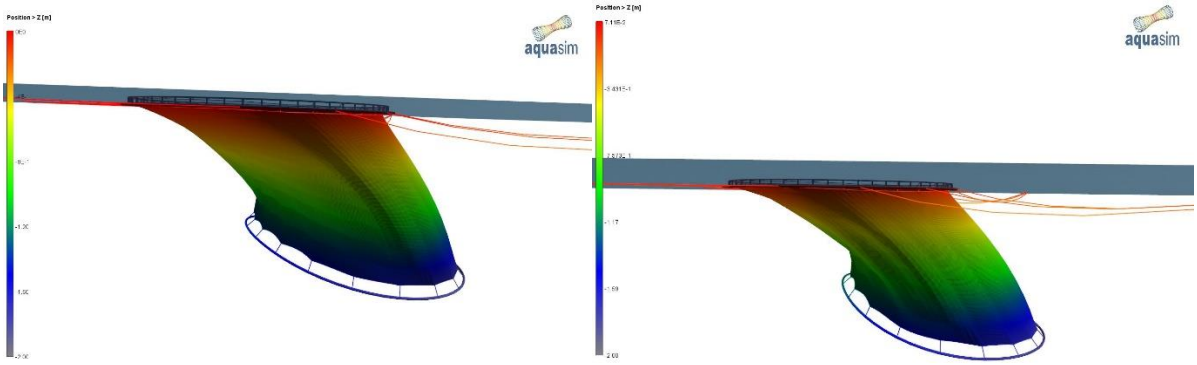

Figure 32 Current velocity 0.193 m/s. Cd 0.8. To the right is a variation where the pressure-coefficient is doubled in the front

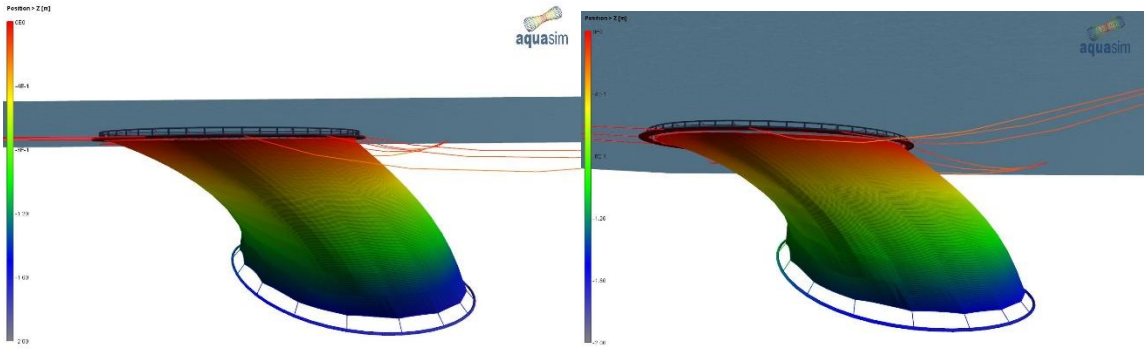

Figure 33 Current velocity 0.193 m/s. Cd 1.0. To the right is a variation where the pressure-coefficient is doubled in the front

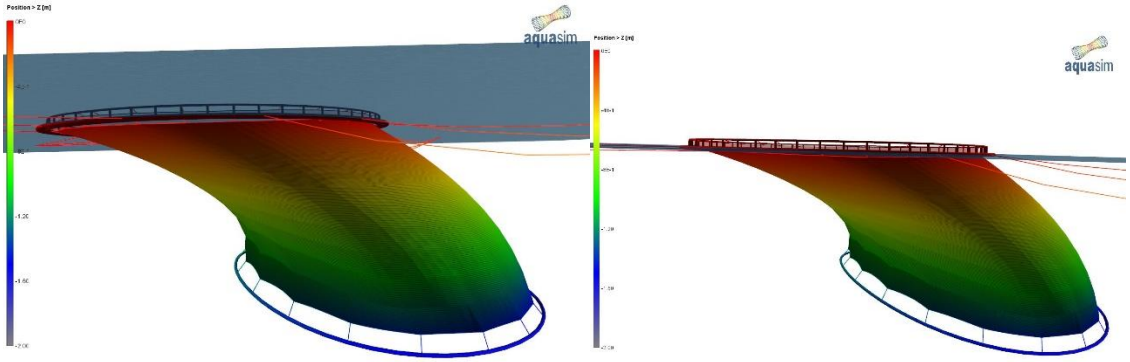

Figure 34 Current velocity 0.193 m/s. Cd 1.2. To the right is a variation where the pressure-coefficient is doubled in the front

As seen by comparing the result in Figure 32 and Figure 34 to the deformed shapes in Figure 27 and Figure 28, it is seen that the case with a drag coefficient of 0.8 to the tarp compares better than the case with a drag coefficient of 1.2. As also seen from Figure 32 the case where the drag has been increased in the front compares even better, but the difference in overall results are not that large so the version with on extra drag in the front has been used as basis for further analysis.

3.3.2. Testing and comparison regular waves with current

The 3 regular waves run in the tank and compared to analysis are shown in Table 3.

Table 3 Cases

	Case 1	Case 2	Case 3
Current velocity [m/s]	0.097	0.145	0.193
Wave amplitude [m]	0.0988	0.0988	0.0988
Wave period, nominal [s]	1.217	1.244	1.271
Wave period earth fixed [s]	1.158	1.158	1.158

Figure 35 shows the response time series of the tree tested conditions.

Figure 35 Time series case 1,2 and 3. The average of the axial load on the left and right load cell on the bridles.

The analysis model values in Table 2. Further parameters for the dynamics are given in Table 4.

Table 4 Parameters on the tube, dynamic analysis base case.

Added mass [mH2O]*	0.28
Damping *$\omega/\rho g$	1
Scaled diffraction MacCamy Fuchs	0.3

**The unit mH2O is "Meters of water".*

Figure 36 shows analysis compared with an excerpt of the test results seen in Figure 35. The following applies for the captions in Figure 36.

- Cd 0.8: Results for analysis with a drag coefficient for the tube, Cd = 0.8
- Cd 1.0: Results for analysis with a drag coefficient for the tube, Cd = 1.0
- Test vs: Results from the tank test, the load cell on the left side, excerpt.
- Test hs: Results from the tank test, the load cell on the right side, excerpt.

In addition to the right of Figure 36, three more results from measurements are presented:

- Test max: Max average of left and right side in the full tank measurement-results seen in Figure 35.
- Test min: Min average of left and right side in the full tank measurement-results seen in Figure 35.
- Test avg.: Min average of left and right side in the full tank measurement-results seen in Figure 35.

3.3.2.1. Case 1

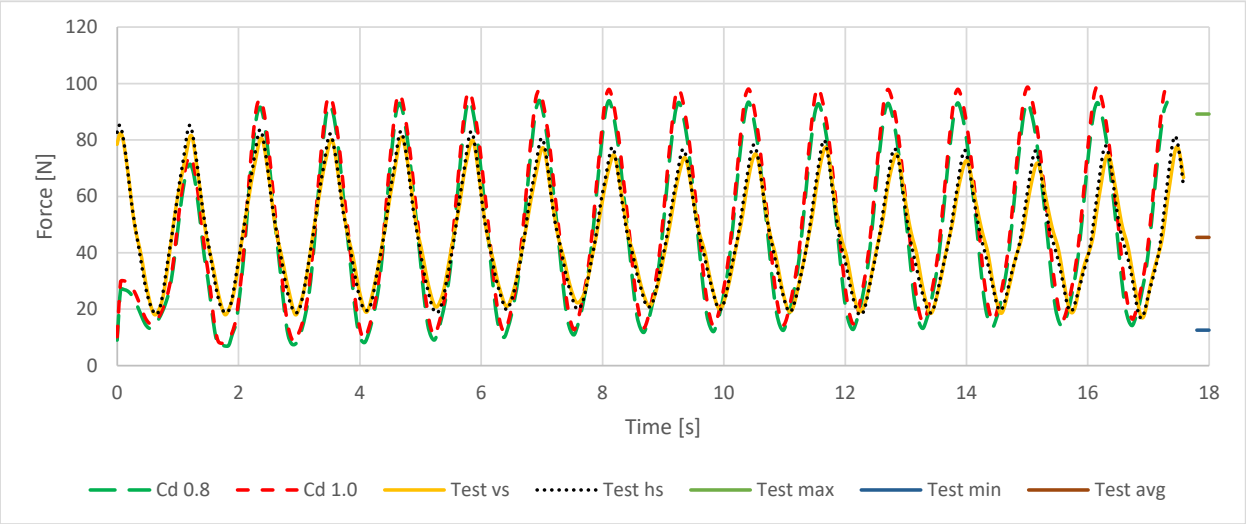

Figure 36 Results case 1.

Figure 37 shows the full time series of test case 1.

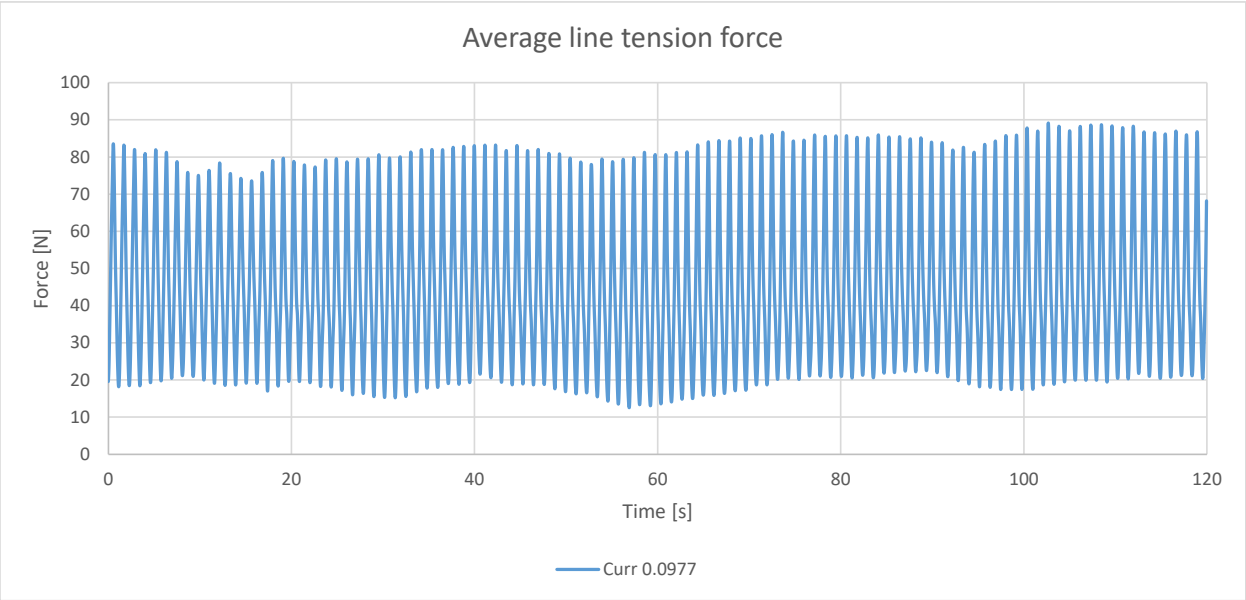

Figure 37 Average line tension force measurements full time series

Table 5 Max, average and mean values compared between analysis and test. In test, the values are the average of the left and right fixation point.

	Cd 0.8	Cd 1.0	Test
Max	94.05	99.41	89.17
Average	48.73	52.49	45.48
min	6.93	7.84	12.52

As seen by comparing analysis and measurements, the results compare well. The max values are lower for the analysis, but in the analysis, the response is a symmetric “steady state” so that when this is compared to the measurements there will be some difference as the response time series seen in Figure 37 there are some more response variations there.

3.3.2.2. Case 2

Figure 38 and Figure 39 shown results for case 2.

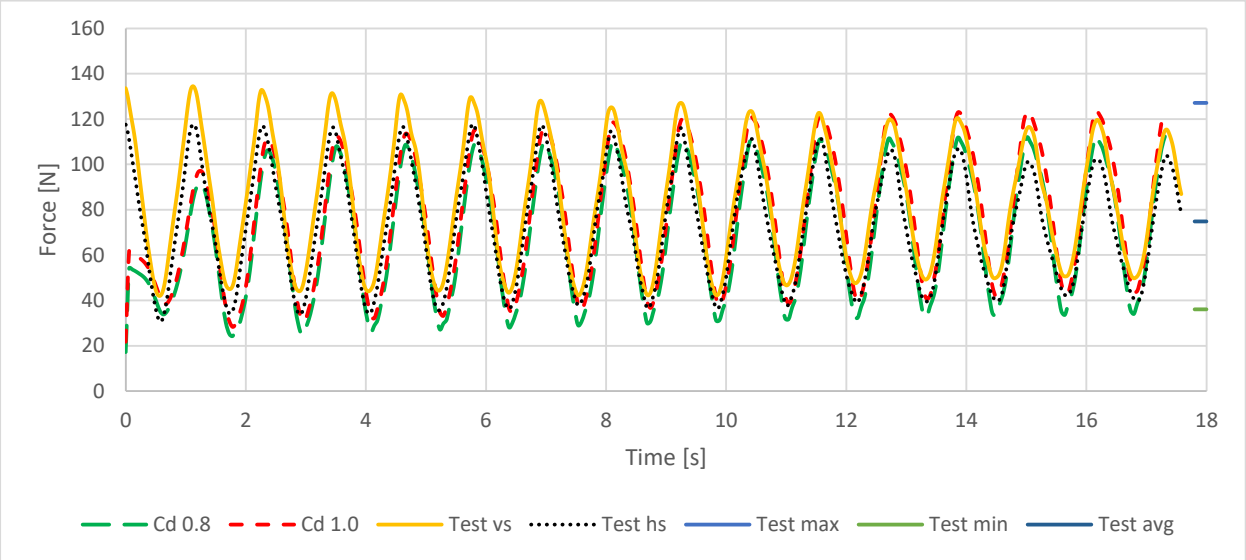

Figure 38 Results case 2.

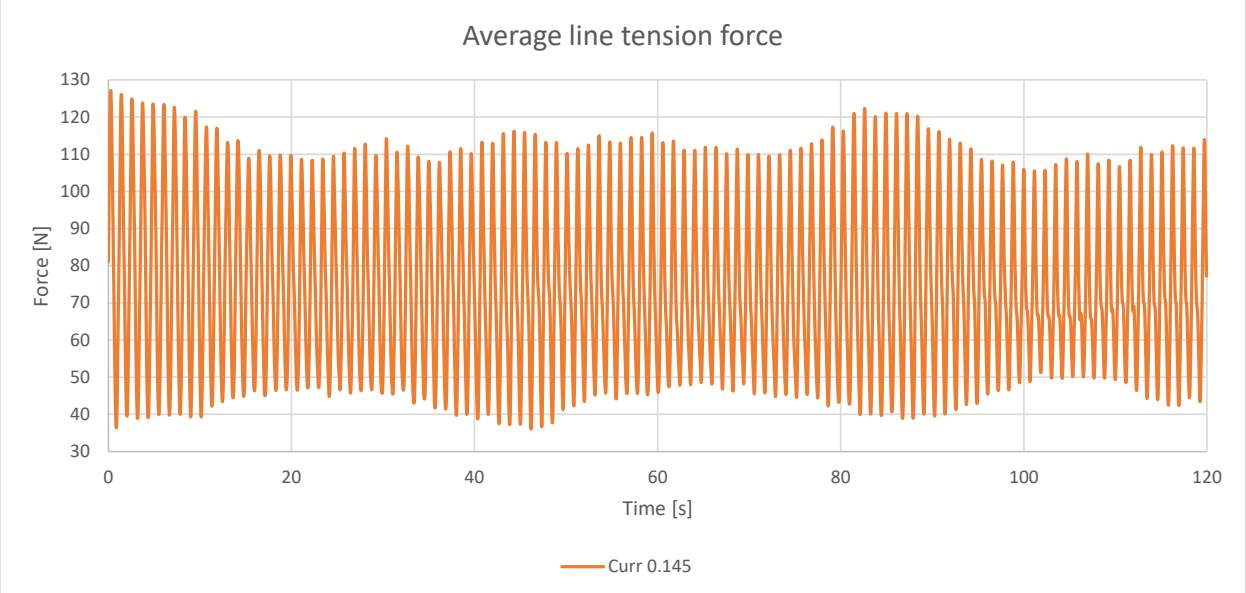

Figure 39 Average line tension force measurements full time series

Table 6 Max, average and mean values compared between analysis and test. In test, the values are the average of the left and right fixation point.

	Cd 0.8	Cd 1.0	Test
Max	112.38	123.74	127.14
Average	70.25	78.75	74.84
min	24.32	28.29	36.09

As seen from Figure 38 and Figure 39 the analysis with these used parameters predicts slightly lower force amplitude than found in the testing but overall correspondence is very well.

3.3.2.3. Case 3

Figure 40 and Figure 41 shows results for case 2.

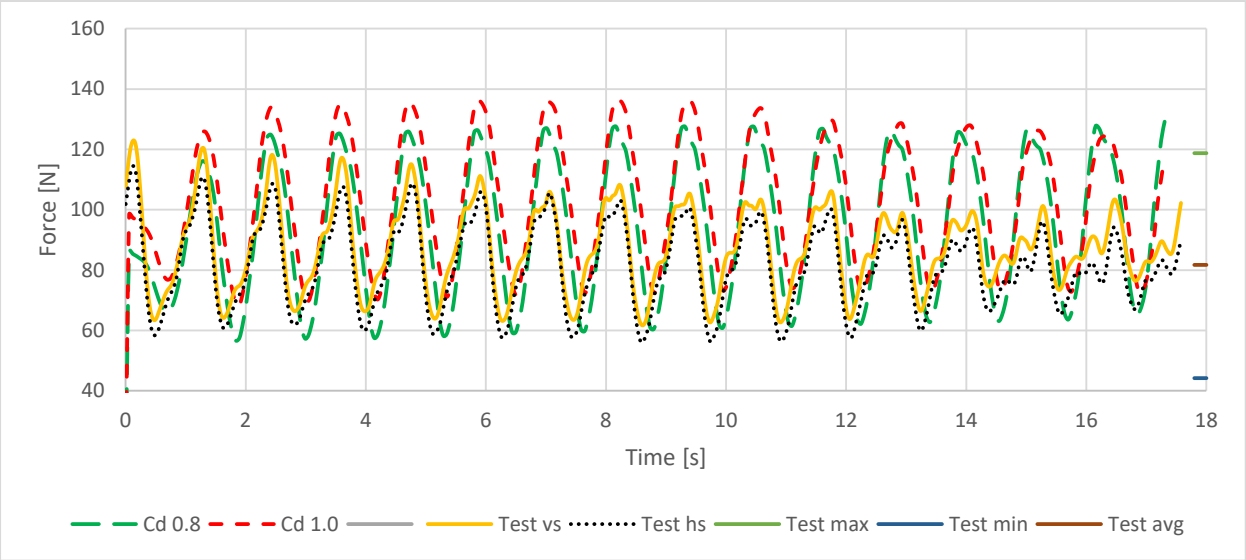

Figure 40 Results case 3

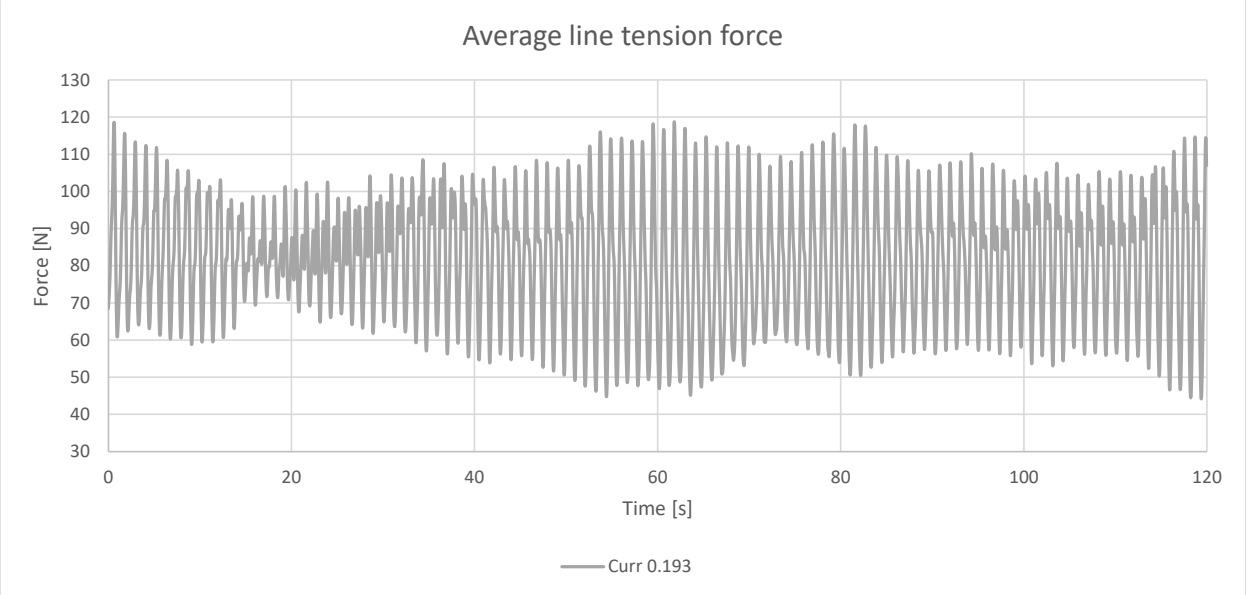

Figure 41 Average line tension force measurements full time series

Table 7 Max, average and mean values compared between analysis and test. In test, the values are the average of the left and right fixation point.

	Cd 0.8	Cd 1.0	Test
Max	129.14	136.33	118.75
Average	95.32	104.21	81.75
min	56.53	68.43	44.20

As seen by comparing analysis and measurements, the results compare well for this case with respect to maximum values, but less well for minimum values and the average.

In real life both drag and lift coefficients as well as other properties such as added mass depends strongly on the condition. This means one cannot assume to choose these values and have good fits for all components.

There are also variations in loading in a tank test and there are uncertainties with respect to modelled parameters. This means one cannot assume a better fit than this. To investigate the influence of parameters a few sensitivity studies has been carried out as reported in the succeeding sections.

3.3.3. Sensitivity of load model

This section investigates the sensitivity to load model where the following apply. The case with Cd 1.0, Added mass has been used for the sensitivity analyse where the captions in Figure 42 – Figure 44 means as follows :

- MF 0.5 : Means that wave loads to the tube has been calculated using 50% flexible tarp load formulation as described in Section 2.4 only combined with 50% MacCamy Fuchs stiff body response.
- MF 0.15 : Means that wave loads to the tube has been calculated using 85% flexible tarp load formulation as described in Section 2.4 only combined with 15% MacCamy Fuchs stiff body response.
- MF 0.3 : The base case using 70% flexible tarp load formulation as described in Section 2.4 only combined with 30% MacCamy Fuchs stiff body response.

Other parameter are the same as in Section 3.3.1 and Section 0.

Figure 42 and Table 8 shows results for case 1.

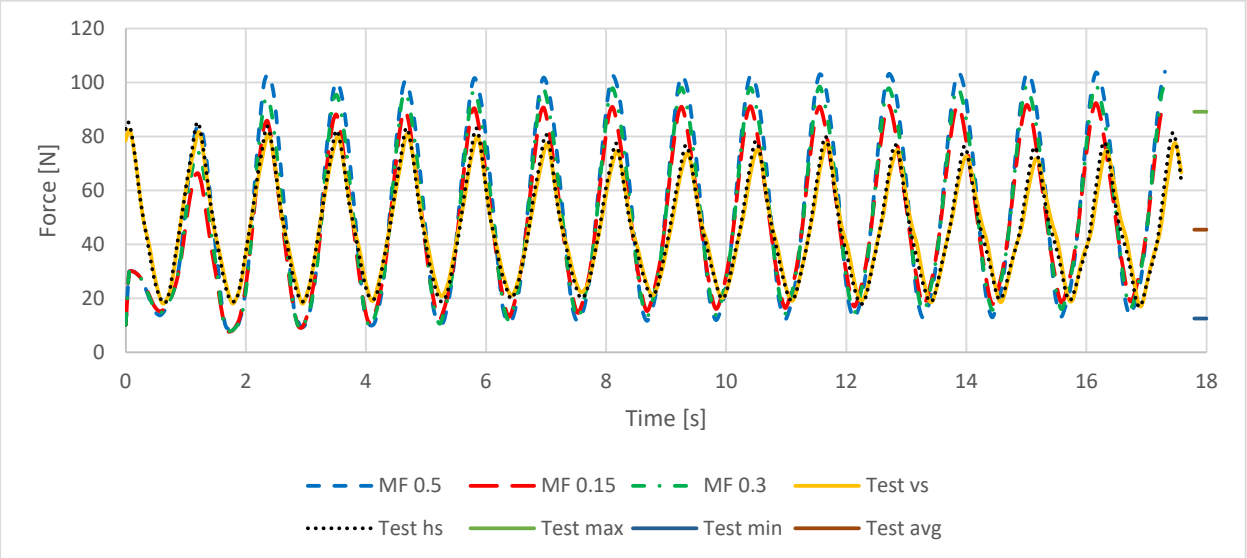

Figure 42 Results case 1

Table 8 Max, average and mean values compared between analysis and test. In test, the values are the average of the left and right fixation point.

	MF 0.5	MF 0.15	MF 0.3	Test
Max	104.03	92.61	99.41	89.17
Average	54.79	49.97	52.49	45.48
min	8.19	7.63	7.84	12.52

Figure 43 and Table 9 shows results for case 2.

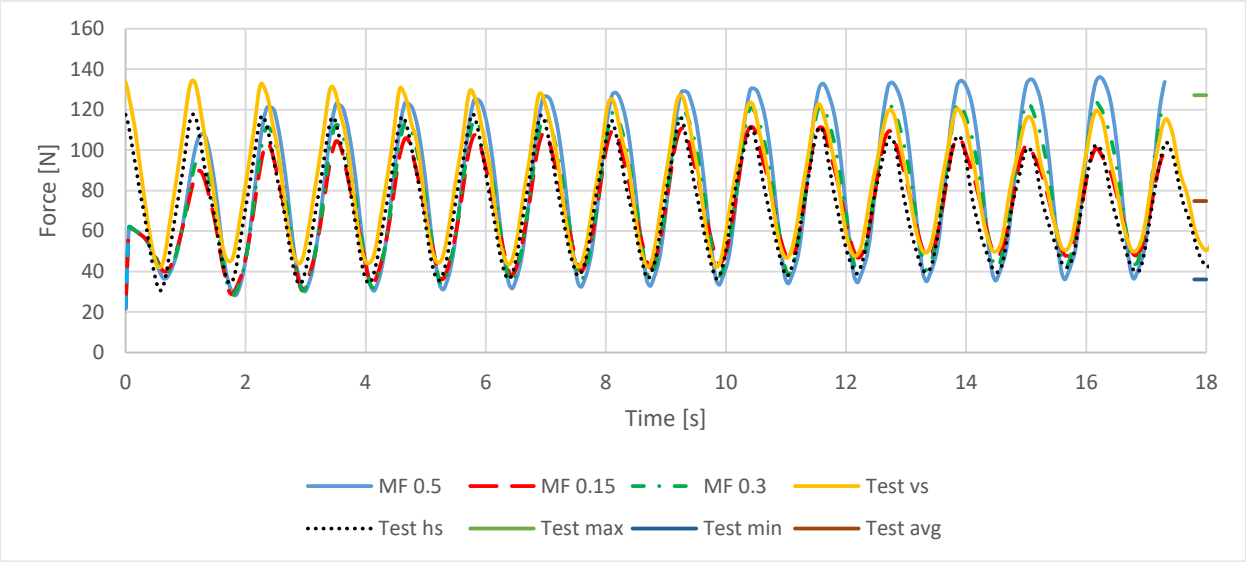

Figure 43 Results case 2

Table 9 Max, average and mean values compared between analysis and test. In test, the values are the average of the left and right fixation point.

	MF 0.5	MF 0.15	MF 0.3	Test
Max	136.08	111.44	123.74	127.14
Average	82.79	73.62	78.75	74.84
min	28.31	28.73	28.29	36.09

Figure 44 and Table 10 shows results for case 3.

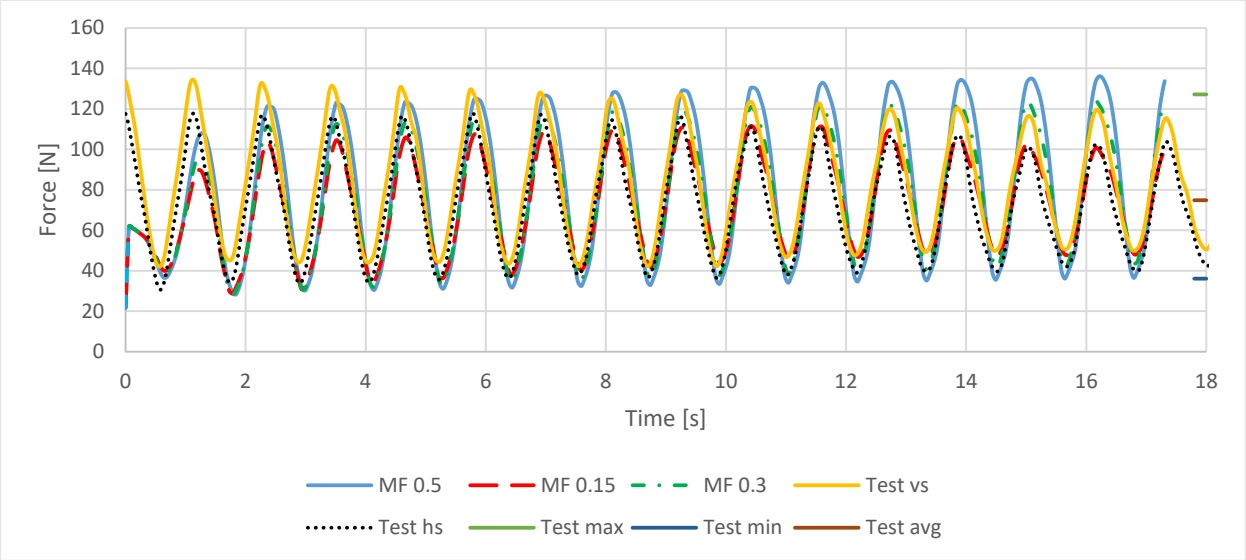

Figure 44 Results case 3

Table 10 Max, average and mean values compared between analysis and test. In test, the values are the average of the left and right fixation point

	MF 0.5	MF 0.15	MF 0.3	Test
Max	160.36	127.12	136.33	118.75
Average	113.55	98.04	104.21	81.75
min	65.18	70.75	68.43	44.20

As seen from this sensitivity study, more diffraction loading the more forces are introduced which is plausible.

3.3.4. Sensitivity of added mass

This section investigates the sensitivity to added mass where the following apply. The case with Cd 1.0, and parameters according to Table 4 while the added mass has been used for the sensitivity analyse where the captions in means as follows :

- Mass 0: Means no added mass.
- Mass 0.28: Means calculations with 0.28 mH20 added mass uniformly around the tube.
- Mass 0.7: Means calculations with 0.7 mH20 added mass uniformly around the tube.

Figure 45 and Table 11 show results case 1.

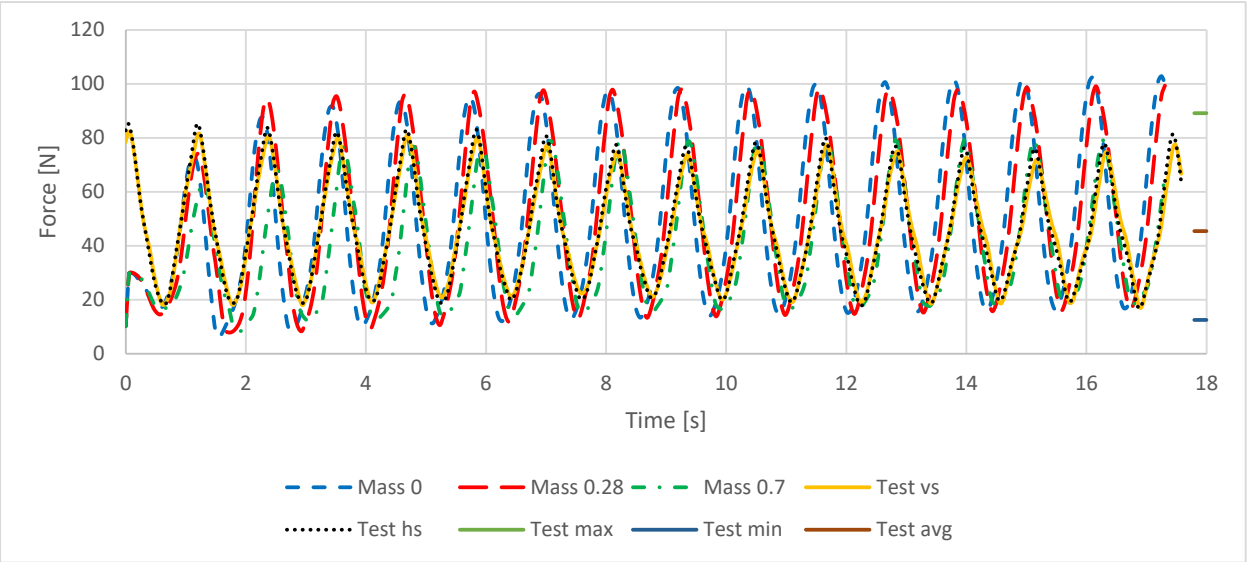

Figure 45 Results case 1

Table 11 Max, average and mean values compared between analysis and test. In test, the values are the average of the left and right fixation point.

	Mass 0	Mass 0.28	Mass 0.7	Test
Max	102.82	99.41	79.38	89.17
Average	51.80	52.49	40.56	45.48
min	5.96	7.84	8.24	12.52

Figure 46 and Table 12 shows results case 2

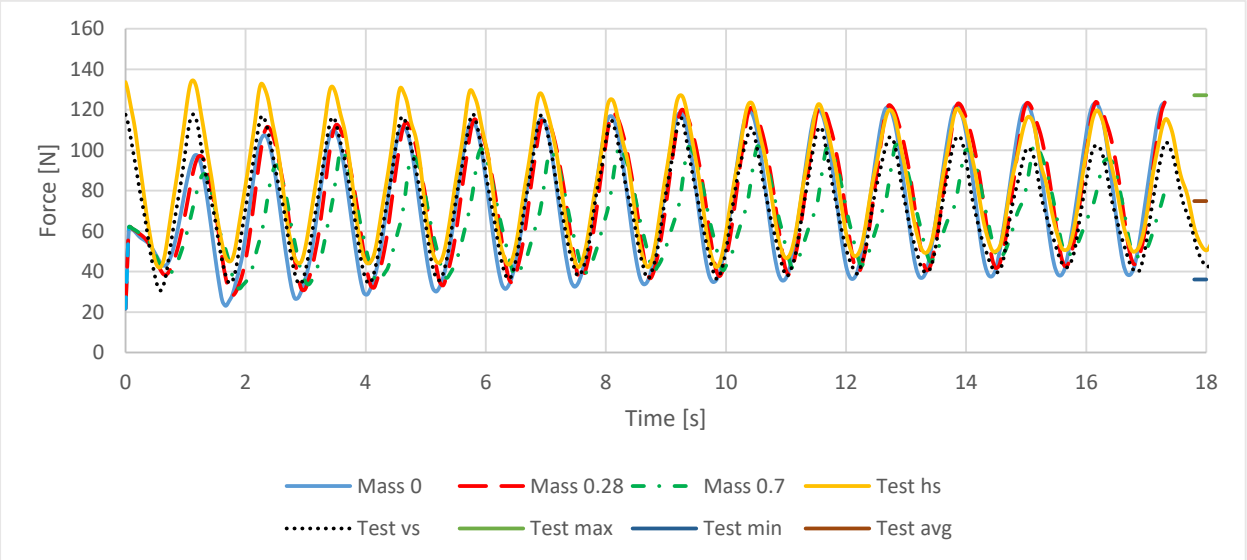

Figure 46 Results case 2

Table 12 Max, average and mean values compared between analysis and test. In test, the values are the average of the left and right fixation point.

	Mass 0	Mass 0.28	Mass 0.7	Test
Max	123.57	123.74	102.46	127.14
Average	74.43	78.75	67.41	74.84
min	23.07	28.29	31.60	36.09

Figure 47 and Table 13 shows results case 3.

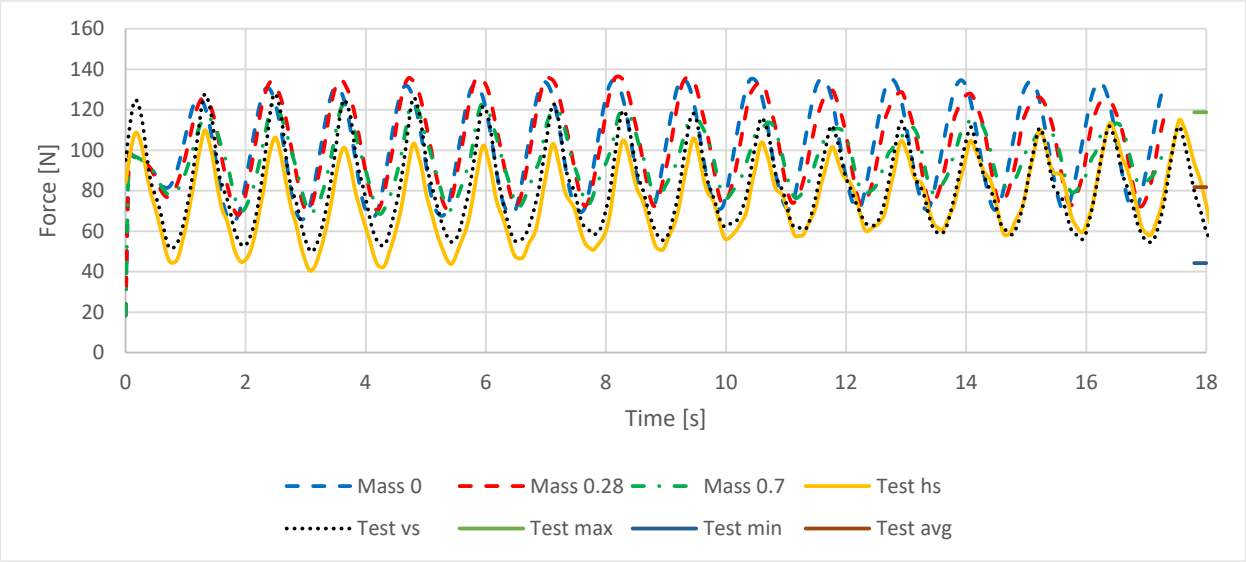

Figure 47 Results case 3

Table 13 Max, average and mean values compared between analysis and test. In test, the values are the average of the left and right fixation point.

	Mass 0	Mass 0.28	Mass 0.7	Test
Max	135.28	136.33	123.56	118.75
Average	101.66	104.21	96.18	81.75
min	64.47	68.43	68.57	44.20

As seen from this sensitivity study less added mass in general increase loading.

3.3.5. Results discussion

Results show that there is good correspondence between the model test, at the numerical formulation with a hybrid solution combining theory for stiff bodies in water.

As a conclusion the parameters for the base case can be chosen for analysis, but to be on the safe side the diffraction theory part of the hybrid load formulation could be increased to 50% and an additional drag effect in front could be considered in the range up to 1 for the extra drag coefficient.

4. CONCLUSION

In AquaSim one may choose from several diffraction theories applicable for calculation on loads to stiff bodies.

Case study 1 and 2 shows the applicability of these theories.

In AquaSim one may also choose a Hybrid load model. Case study 3 shows that this hybrid model is applicable for flexible tubes.

Parameters are shown and the effect of loading. What parameters to use for design should be chosen combined with how much other knowledge there is about the system such that conservatism is secured.

In general, the more load application is based on the stiff body response diffraction theory the higher loads are calculated as compared to the free tarp theory. Hence using the hybrid model for a flexible system, one should have supporting test data to choose the flexible tarp part of the load higher than 50 %.

Applicable added mass is a complex issue and sensitivity studies should be considered in case of resonance or susceptibility to impact load response.

5. REFERENCES

Aquastructures (2012) “Verification and benchmarking of AquaSim, a softwaretool for safety simulation of flexible offshore facilities exposed to environmental and operational loads“, Aquastructures report 2012-1755-1.

Aquastructures (2013) “The AquaSim Package user manual” Aquastructures report TR-30000-2049-1.

Aquastructures (2013b) “On the analysis of moored lagre mass floating objects and how to carry out such analysis with AquaSim” Aquasim report NO. 2174-1. Revision NO. 02.

Aquastructures (2016) “Impermeable nets in AquaSim” TR-FOU-2692-2. Aquastructures 2016

Babarit, A., G. Delhommeau (2015): Theoretical and numerical aspects of the open source BEM solver NEMOH. In Proc. of the 11th European Wave and Tidal Energy Conference (EWTEC2015), Nantes, France.

Barkley, D (2006) "Linear analysis of the cylinder wake mean flow" Europhys. Lett., 75 (5), pp. 750–756 (2006) DOI: 10.1209/epl/i2006-10168-7

Berstad, L.F. Heimstad (2015) “Numerical Formulation of Sea Loads to Impermable nets” VI International Conference on Computational Methods in Marine Engineering.MARINE 2015, Rome, Italy.

Egesund net (2020) “AquaSim vs. modellforsøk - 90x20 m tube i strøm og bølger” Author Ketil Roaldsnes. Date 21.03.2020. Egersund net.

Faltinsen, Odd M. (1990) “Sea loads on ships and offshore structures.” Cambridge university press ISBN 0 521 37285 2

McCamy, R. and R. Fuchs (1954), Wave forces on piles: a diffraction theory. Tech. Memo No. 69, U.S. Army Corps of Engrs, 1954.

MDP (2020) http://www-mdp.eng.cam.ac.uk/web/library/enginfo/aerothermal_dvd_only/aero/fprops/poten/node37.html .

Morison, J, M.O’Brien, J. Johnson and S. Shaff (1950). “The forces Exerted by surface waves on piles.” Petrolium Trans. 189, 149-1.

Ogawa, S. and Kimura, Y. (2018) «Performance Improvement by Control of Wingtip Vortices for Vertical Axis Type Wind Turbine.» Open Journal of Fluid Dynamics, 8, 331-342. https://doi.org/10.4236/ojfd.2018.83021

Sintef (2020) "The North Sea Centre Flume Tank" SINTEF Fisheries and Aquaculture, The North Sea Centre, P.O. Box 104, DK-9850 Hirtshals, Denmark. https://www.sintef.no/globalassets/upload/fiskeri_og_havbruk/faktaark/flumetank_eng.pdf

- o0o -